Simulated and Observed Circulation in the Indonesian Seas: 1/12° Global HYCOM and the INSTANT Observations

E.J. Metzger[a], H.E. Hurlburt[a], X. Xu[b], Jay F. Shriver[a], A.L. Gordon[c], J. Sprintall[d], R.D. Susanto[c] and H.M. van Aken[e]

[a]Naval Research Laboratory
Stennis Space Center, Mississippi, 39529-5004 USA
joe.metzger@nrlssc.navy.mil
harley.hurlburt@nrlssc.navy.mil
jay.shriver@nrlssc.navy.mil

[b]Department of Marine Science
The University of Southern Mississippi
1020 Balch Blvd.
Stennis Space Center, Mississippi, 39529 USA
xiaobiao.xu@usm.edu

[c]Lamont-Doherty Earth Observatory
Earth Institute at Columbia University
61 Route 9W
Palisades, New York, 10964-1000 USA
agordon@ldeo.columbia.edu
dwi@ldeo.columbia.edu

[d]Scripps Institution of Oceanography
University of California San Diego
9500 Gillman Drive
La Jolla, California, 92093 USA
jsprintall@ucsd.edu

[e]NIOZ Royal Netherlands Institute for Sea Research
Texel, The Netherlands
aken@nioz.nl

Corresponding author: E. Joseph Metzger, NRL Code 7323, Stennis Space Center, MS, 39529, (228) 688-4762 (office), (228) 688-4759 (fax), joe.metzger@nrlssc.navy.mil

14 April 2010

Report Documentation Page

Form Approved
OMB No. 0704-0188

1. REPORT DATE	2. REPORT TYPE	3. DATES COVERED
14 APR 2010		**00-00-2010 to 00-00-2010**

4. TITLE AND SUBTITLE	5a. CONTRACT NUMBER
Simulated and Observed Circulation in the Indonesian Seas: 1/12degree Global HYCOM and the INSTANT Observations	5b. GRANT NUMBER
	5c. PROGRAM ELEMENT NUMBER
6. AUTHOR(S)	5d. PROJECT NUMBER
	5e. TASK NUMBER
	5f. WORK UNIT NUMBER
7. PERFORMING ORGANIZATION NAME(S) AND ADDRESS(ES) **Naval Research Laboratory,Stennis Space Center,MS,39529-5004**	8. PERFORMING ORGANIZATION REPORT NUMBER
9. SPONSORING/MONITORING AGENCY NAME(S) AND ADDRESS(ES)	10. SPONSOR/MONITOR'S ACRONYM(S)
	11. SPONSOR/MONITOR'S REPORT NUMBER(S)

12. DISTRIBUTION/AVAILABILITY STATEMENT
Approved for public release; distribution unlimited

13. SUPPLEMENTARY NOTES

14. ABSTRACT
see report

15. SUBJECT TERMS

16. SECURITY CLASSIFICATION OF:			17. LIMITATION OF ABSTRACT	18. NUMBER OF PAGES	19a. NAME OF RESPONSIBLE PERSON
a. REPORT **unclassified**	b. ABSTRACT **unclassified**	c. THIS PAGE **unclassified**	**Same as Report (SAR)**	**61**	

Abstract

A 1/12° global version of the HYbrid Coordinate Ocean Model (HYCOM) using 3-hourly atmospheric forcing is analyzed and directly compared against observations from the International Nusantara STratification ANd Transport (INSTANT) program that provides the first long-term (2004-2006) comprehensive view of the Indonesian Throughflow (ITF) inflow/outflow and establishes an important benchmark for inter-basin exchange, including the net throughflow transport. The simulated total ITF transport (-13.4 Sv) is similar to the observational estimate (-15.0 Sv) and correctly distributed among the three outflow passages (Lombok Strait, Ombai Strait and Timor Passage). Makassar Strait carries ~75% of the observed total ITF inflow and while the temporal variability of the simulated transport has high correlation with the observations, the simulated mean volume transport is ~37% too low. This points to an incorrect partitioning between the western and eastern inflow routes in the model and is the largest shortcoming of this simulation. HYCOM simulates the very deep (>1250 m) overflow at Lifamatola Passage (-2.0 Sv simulated vs. -2.5 Sv observed) and indicates overflow contributions originating from the North (South) Equatorial Current in boreal winter-spring (summer-autumn). A new finding of INSTANT is the mean eastward flow from the Indian Ocean toward the interior Indonesian Seas on the north side of Ombai Strait. This flow is not robustly simulated at 1/12° resolution, but is found in a 1/25° version of global HYCOM using climatological forcing, indicating the importance of horizontal resolution. However, the 1/25° model also indicates that the mean eastward flow retroflects, turning back into the main southwestward Ombai Strait outflow, and in the mean does not enter the interior seas to become part of the water mass transformation process. The 1/12° global HYCOM is also used to fill in the gaps not measured as part of the INSTANT observational network. It indicates the wide and

shallow Java and Arafura Seas carry -0.8 Sv of inflow and that the three major outflow passages capture nearly all the total Pacific to Indian Ocean throughflow.

Keywords: Indonesian Throughflow, global HYCOM, INSTANT, inter-ocean exchange, ocean modeling

1. Introduction

The Indonesian Seas lie in a major cross-road of the global ocean circulation and act as a chokepoint with global-scale impact. The flow through these seas, generally from the Pacific to the Indian Ocean, is known as the Indonesian Throughflow (ITF) and its transport can have significant impacts on the temperature (T) and salinity (S) structure of the Indian Ocean. The unique waters of North and South Pacific origin that enter this "mix-master" region, clearly exit as Indonesian waters (Gordon, 2005) and can have downstream influences as far as the Agulhas Retroflection region.

The expansive and complex island/strait geometry has made this a difficult region to take comprehensive observational measurements of the ITF. Prior to 2004, the various outflow passages of Lombok Strait (Murray and Arief, 1988), Ombai Strait (Molcard et al., 2001) and Timor Passage (Cresswell et al., 1993; Molcard et al., 1994; Molcard et al., 1996) (Fig. 1) had not been contemporaneously observed. This is problematic because Meyers (1996) and Potemra and Schneider (2007) (among others) indicate the ITF varies with the different phases of the El Niño-Southern Oscillation (ENSO). The International Nusantara STratification ANd Transport (INSTANT) program (Sprintall et al., 2004) was thus designed to mitigate the previous lack of simultaneous temporal sampling and the analyzed results of these observations are reported on in this issue (Gordon et al., 2010, Sprintall et al., 2010) and elsewhere. Spanning the 2004-2006

time frame, the INSTANT observations provide the first long-term comprehensive view of the ITF inflow/outflow and furnish an important benchmark for observationalists and modelers alike.

While the INSTANT observations provide the best observational estimate of ITF transport to date, it is limited to the five instrumented passages. Apart from a few very shallow and narrow straits that are thought not to carry a substantial amount of transport, the outflow passages (Lombok Strait, Ombai Strait and Timor Passage) are well resolved by INSTANT (Sprintall et al., 2009). This is also true for Makassar Strait, which carries the majority of the ITF inflow (Gordon et al., 2008). However, in the passages east of Sulawesi, only a single mooring was deployed and it was designed to measure the deep overflow at Lifamatola Passage (van Aken et al., 2009). The expanse of the region and configuration of the islands does not easily lend itself to monitoring these eastern passages. Likewise, observing the flow through the relatively shallow Java and Arafura Seas (via Karimata and Torres Straits, respectively) was not part of the INSTANT network. Although shallow, these seas are rather wide and together their contribution to the total ITF inflow transport has not been adequately observed.

Accurate simulation of the circulation in the Indonesian Seas and the ITF also has historically been a very challenging problem for numerical ocean modelers. Relatively high horizontal resolution is required (probably 1/10° or finer) to represent many of the very narrow straits and passages. The computational resources exist such that sufficient resolution can easily be obtained using a regional ocean general circulation model (OGCM), but the ITF transport is ultimately governed by the outer boundary conditions, whether these come from a coarser resolution global model or from climatology. In either case, the ITF transport is imposed upon the nested model. Thus, a global model is needed with high horizontal resolution in the Indonesian Seas. This can come from a telescoping grid that focuses on the region, or by having

high horizontal resolution globally (the approach used in this paper). In addition to the coastline geometry, topographic databases that accurately define the sill depths in the key passages must be interpolated to the OGCM grid.

The INSTANT program has established a very important benchmark with regard to the ITF transport and has furthered our knowledge of the vertical structure of the flow at the key straits in the Indonesian Seas. It is also a benchmark that cannot be ignored by ocean modelers as it significantly reduces the error bounds of the Pacific to Indian Ocean Throughflow. Thus, one of the motivations of this paper is a baseline comparison of INSTANT observations with the eddy-resolving 1/12° global version of the HYbrid Coordinate Ocean Model (HYCOM) integrated over the same time period. We focus on integrated transport and the velocity structure at the INSTANT mooring locations and do not place much emphasis on the temperature and salinity characteristics at this time. Careful analysis and comparison of the observations to the numerical output will provide crucial knowledge about the realism of the simulation that should lead to a better understanding on how to improve model physics, as well as the sensitivity to the passage topography, geometry and sill depths. Another motivation is to use HYCOM to complement the INSTANT observations and provide a larger scale context of the circulation pathways in the region. For example, what is the distribution of Makassar Strait transport coming from Sibutu Passage versus via the Sulawesi Sea? Or, what are the source regions of the deep Lifamatola Passage overflow? A final motivation is to use the numerical model to fill in gaps within the INSTANT network. The array of moorings was limited to the key passages assuming the secondary throughflow routes (via the Java or Arafura Seas) were negligible. Global HYCOM is used to show how the transport through the shallow Karimata and Torres Straits fits into the

overall ITF budget, in addition to the contribution of several gaps along the Nusa Tenggara archipelago.

The paper is divided into six sections. After this introduction, the numerical ocean model is described in section 2. This is followed by a section on the main model-data comparisons. Section 4 is focused on the circulation pathways in 1/12° global HYCOM and section 5 addresses how the model can be used to fill in the gaps of the observational network. Lastly, we end with a discussion and summary.

2. Numerical model description

HYCOM is a community ocean model (http://www.hycom.org) that utilizes generalized vertical coordinates (Bleck, 2002). Although not limited to these types, typically the vertical coordinates are isopycnals (density tracking), best used in the stratified deep ocean, levels of equal pressure (nearly fixed depths), best used in the mixed layer and unstratified ocean, or σ-levels (terrain-following), often the best choice in shallow water (Chassignet et al., 2003). HYCOM combines all three approaches by choosing the optimal distribution at every time step. The model makes a dynamically smooth transition between coordinate types by using the layered continuity equation. The hybrid coordinate extends the geographic range of applicability of traditional isopycnic coordinate circulation models toward shallow coastal seas and unstratified parts of the world ocean. It maintains the significant advantages of an isopycnal model in stratified regions while allowing more vertical resolution near the surface and in shallow coastal areas, hence providing a better representation of the upper ocean physics.

This version of HYCOM has horizontal equatorial resolution of 1/12.5º cos(lat) x 1/12.5º (latitude x longitude) (hereafter, simply 1/12°) or slightly finer than 9 km within the Indonesian

Seas. The fully global grid is on a Mercator projection from 78.64ºS to 47ºN and north of this it employs an Arctic dipole patch where the poles are shifted over land to avoid a singularity at the North Pole. It employs 32 hybrid vertical coordinate surfaces with potential density referenced to 2000 m and it includes the effects of thermobaricity (Chassignet et al., 2003). The layer structure is chosen to have sufficient resolution in the mixed layer (typically in z-space) and increasingly thicker isopycnal layers with depth. HYCOM is configured with options for a variety of mixed layer sub-models (Halliwell, 2004) and this version uses the NASA Goddard Institute for Space Studies (GISS) level 2 turbulence closure model (Canuto et al., 2001; 2002).

As indicated above, the representation of the coastlines and bottom topography is very important in this region. However, our experience has been that all topographic databases need substantial hand-editing and we have used a combination of navigational charts and the scientific literature to accomplish this. The Naval Research Laboratory (NRL) 2' Digital Bathymetric Data Base 2 (DBDB2) (Ko, 2002) was interpolated to the HYCOM grid and one pass of a 9-pt smoother was applied to prevent the generation of numerical noise at very small scales. A consequence of the smoothing is to shallow trenches and reduce the amplitude of seamounts. Significant hand-editing was performed globally on the representation of the coastlines, such as, defining the proper widths of straits or making sure some misplaced islands were correctly co-located on its corresponding seamount. In addition, the INSTANT web site (http://www.marine.csiro.au/~cow074/) and the scientific literature were used to determine the sill depths in the key passages and hand-edits were performed at these locations. However, in an unfortunate oversight, the model topography with *edited* coastlines but *unedited* sill depths was used and only discovered after the completion of the multi-year integration. Thus, the sill depths used in HYCOM are generally too shallow compared to the observed estimates and these are

defined in Table 1. While there is an overall shallow bias to the model topography, HYCOM adequately simulates the ITF because ~2/3 of the transport occurs in the upper 300 m of the water column (Sprintall et al., 2009). It is also consistent with the results of Potemra (2005) who shows that 83% of the total ITF transport occurs above 200 m in the Simple Ocean Data Assimilation model. As will be discussed below, incorrect model depths at Dewakang Sill in the southern Makassar Strait present the largest problem. We have since used the Smith and Sandwell (1997) 1' topography to correct the model depths.

The model was initialized using T and S from the Generalized Digital Environmental Model (GDEM) Version 3.0 climatology (Carnes, 2009) and was spun-up for thirteen model years using a monthly climatology based on the 1979-93 1.125° European Centre for Medium-Range Weather Forecasts (ECMWF) first reanalysis (ERA15) (Gibson et al, 1999). The forcing includes: air temperature at 2 m, surface specific humidity, net surface shortwave and longwave radiation, total (large-scale plus convective) precipitation, ground/sea temperature, zonal and meridional wind velocities at 10 m, mean sea level pressure and dewpoint temperature at 2 m. The first six fields are either input directly into the ocean model or used in calculating components of the heat and buoyancy fluxes, while the last four fields are used to compute surface wind stress with temperature and humidity based stability dependence (Kara et al., 2005). After spin-up, the model used the Fleet Numerical Meteorology and Oceanography Center (FNMOC) 3-hourly 0.5º Navy Operational Global Atmospheric Prediction System (NOGAPS) forcing (Rosmond et al., 2002) spanning the time frame January 2003-April 2007. For the wind forcing, the long-term (annual) mean from NOGAPS was replaced by the ERA15 mean for consistency on the large scale as this prevents any spin up/down due to differences in the two global wind products. Thus the long-term mean is still driven by ECMWF while the interannual,

monthly, and sub-monthly fluctuations are driven by NOGAPS. The temporal resolution of the wind forcing is 3-hourly, but the thermal forcing has been daily averaged.

No oceanic data are assimilated into this version of HYCOM, except that sea surface salinity (SSS) is relaxed to the Polar Science Center Hydrographic Climatology (Steele et al., 2001). This is required to prevent long-term SSS drift due to inadequate precipitation minus evaporation forcing. In addition, monthly varying discharge from nearly 1000 rivers (Barron and Smedstad, 2002) is included as a surface precipitation flux (but not as a volume flux).

Internal tides and the associated vertical mixing are responsible for water mass transformation within the Indonesian Seas as suggested by observations (Ffield and Gordon, 1996) and as demonstrated using regional models of this area (e.g. Robertson and Ffield, 2005 and Koch-Larrouy et al., 2007). Vertical mixing associated with tides has been parameterized in some global OGCMs and has demonstrated an impact on the T and S structure (e.g. Lee et al., 2006 in the North Atlantic), but we are aware of only one global OGCM where tidal forcing is explicitly included and the impact in the ITF region has been examined, i.e. Schiller (2004) and Schiller and Fiedler (2007) using various versions of the Modular Ocean Model (MOM). In the former study tides were implemented regionally in the Indonesian Seas. With relatively coarse resolution (0.5° longitude x 0.33° latitude) Schiller (2004) clearly states that internal tides are not properly resolved, but believes the parameterizations for tidally induced mixing are appropriate enough to simulate the effect. Compared to the case without tidal forcing, he noted a 4.5 Sv increase in ITF transport along the WOCE IX1 section in the simulation with tides. However, the grid representation of some narrow passages (Lombok and Malacca Straits) was much larger than observed and so the pathways within the interior seas may not be realistic. In the latter study, tides were implemented globally (including phase information) and the horizontal

resolution is high (0.1°) in a 90° sector around Australia that includes the Indonesian Seas. Those model results suggest large tide-induced mixing in some narrow straits. An initial attempt has been made to implement the 8 largest tidal constituents in 1/12° global HYCOM, where mixing associated with topographic wave drag over rough topography is parameterized (Arbic et al., 2010). The impact of adding tides was increased transport through Makassar Strait (a result consistent with Schiller (2004)) but we note a net reduction of total ITF transport by ~2 Sv (as measured at the outflow passages). In the Indonesian Seas, the model generates strong internal tides and the surface tides appear to be reasonable, but some near-bottom, unphysical gyres occur in the model solution where the topographic wave drag is high. Thus we exclude any discussion of tidal impacts in this manuscript as their implementation is not mature enough in HYCOM.

HYCOM output consists of daily instantaneous snapshots at 00Z saved as archive files on the native hybrid vertical coordinate. For some analyses, the output was remapped in the vertical to fixed z-levels using linear interpolation between cell centers. The vertical remapping was not very sensitive to the interpolation method. The INSTANT instruments at the various mooring sites had slight variations of their actual time in the water, but we used 1 January 2004 – 31 December 2006 as the simulated three year INSTANT time period. The simulation ran on the IBM Power 4+ at the Navy DoD Supercomputing Resource Center (Stennis Space Center, MS) using 781 processors and took approximately 23 wall-clock hours per model month of integration.

The discussion above describes the main simulation used throughout this manuscript; however, a few supplementary simulations are also used. These experiments are spun-up with the second ECMWF reanalysis (ERA40, Kallberg et al., 2004) 1.125° 1979-2002 climatological forcing using the bulk formulation of Kara et al. (2005) for converting 10 m winds to wind stress

and with the wind speeds corrected using a regression to a monthly climatology from the QuikSCAT scatterometer data (Kara et al., 2009), i.e. ERA40-QuikSCAT. In general, the numerical weather prediction wind speeds are increased across the globe but exhibit regional variability. Simulations forced by this product are typically closer to a broad set of metrics used to validate the model. In addition, Kara et al. (2009) showed the QuikSCAT correction led to reduced simulated SST error in the Mediterranean Sea. The model topography in some of these supplementary simulations also has more accurate sill depths in the key passages, namely Sibutu Passage, Sangihe Ridge, Halmahera Sea, Dewakang Sill, Lifamatola Passage, Ombai/Wetar Strait, Timor Passage, Savu Strait, Sumba Strait and Lombok Strait.

3. Global HYCOM comparisons with the INSTANT observations

3.1 Total transport

The zero order comparison between global HYCOM and the INSTANT observations is an examination of the simulated volume transport with regard to the circulation pathways (Fig. 2). Sprintall et al. (2009) sum the three outflow passages of Lombok Strait, Ombai Strait and Timor Passage to obtain their best estimate of total ITF transport spanning the 2004-2006 INSTANT time frame, which is -15.0 Sv (1 Sverdrup = 10^6 m^3/s) (negative transport is defined as from the Pacific Ocean into the Indian Ocean). Depending upon how the observations were extrapolated to the surface and sidewalls, the range expands to -10.7 to -18.7 Sv. Summing the same three outflow passages, global HYCOM simulates a net ITF transport of -13.4 Sv. The model shows good agreement in total transport at Lombok and Ombai Straits, but simulates lower than observed transport at Timor Passage.

In their Appendix A.2, Metzger and Hurlburt (1996) discuss a quantitative relationship for geostrophic versus hydraulic control of transport through a strait, including contributions to hydraulic control from both Bernoulli setdown and bottom friction. In addition, they tested this theory in Sibutu Passage and the Java Sea using a numerical model. Wijffels et al. (2008) use this type of concept to hypothesize that the flow through the relatively shallow Lombok Strait (300 m sill depth) must be dynamically saturated either by hydraulic control or friction, forcing the excess through Ombai. They continue that the same saturation must also be true for Ombai due to the existence of Timor throughflow above the controlling sill depth (1150 m) in the Savu Sea. The simulated total ITF transport is 1.6 Sv less than observed, all of which is missing at Timor Passage, suggesting saturated flow at Lombok and Ombai Straits in HYCOM as well.

Gordon et al. (2008) report -11.6 Sv through Makassar Strait, which accounts for 77% of the ITF. This remains consistent with Gordon (2005) that indicated Makassar carries ~80% of the ITF based on earlier observational studies. The simulated Makassar Strait transport is only -7.3 Sv, or 54% of the total ITF. Reasons for this large discrepancy between the model and observed transport will be discussed below. The deep overflow transport at Lifamatola Passage (>1250m) reported by van Aken et al. (2009) is -2.5 Sv and HYCOM simulates -2.0 Sv. The vertical structure of transport is illustrated in Fig. 3 and overall HYCOM compares well with the INSTANT observations.

3.2 Makassar Strait

The largest transport differences between the observations and the model are at Makassar Strait (Fig. 3a). Within the top 300 m, simulated transport is 1.3 Sv too weak, but 3.0 Sv too weak between 400-1500 m. As indicated in Table 1, the observed and model sill depths differ by

195 m at Dewakang Sill (Fig. 1 inset), located near the southern end of the strait. HYCOM has significantly reduced southward flow over this depth range suggesting that inaccurate model topography is one of the reasons for the reduced transport. Subsequent 1/12° global HYCOM simulations with identical *climatological* ERA40-QuikSCAT forcing using the same topography as the main experiment and a second simulation using a modified topography to more accurately reflect the sill depths in all the key passages indicate the ratio of Makassar Strait transport to the total ITF transport increases from 60% to 67%, respectively. Fifty-nine percent of this transport change came within the depth range between ~450-650 m, i.e. those layers that were blocked by the model sill before the topography modification, but open after modification to the model sill at Dewakang. Thus, the topography changes have moved the ratio more in line with the observations and highlight the importance of accurate model topography to properly simulate the circulation pathways.

Both the observed and simulated velocity components have been rotated to be in line with the direction of the flow through the strait, i.e. the along strait velocity (ASV). A model-data comparison of ASV profiles for the long-term mean, northwest monsoon (January-February-March [JFM]) and southeast monsoon (July-August-September [JAS]) seasons (Fig. 4) shows the Makassar Strait profiles are quite similar, although the simulated maximum southward flow is deeper than observed. The observed thermocline ASV depth of maximum velocity/maximum velocity varies between 140 m/66.5 cm/s in JFM and 110 m/57.8 cm/s in JAS, whereas it is 160 m/60.7 cm/s and 160 m/62.3 cm/s, respectively, in global HYCOM. Just as the simulated transport vs. depth (Fig 3a) is too weak in the top two slabs and below 300 m, so too is the simulated ASV in these depth ranges. Gordon et al. (2008) notes that the relative strengths of the

JFM and JAS ASV profiles reverse around 220 m; HYCOM shows a similar reversal albeit shallower in the water column (~185 m) (Fig. 4b).

While the simulated mean transport through Makassar Strait is weak compared to the observations, the interannual variability is quite similar (Fig. 5) and the two time series have a correlation coefficient of 0.74. Gordon et al. (2008) notes the observed transport minima during the monsoon transition seasons (May 2004 and 2005, November 2004, 2005 and 2006) appear to be associated with coastally-trapped Kelvin waves propagating eastward along Sumatra coast, entering Lombok Strait and continuing into Makassar Strait, as hypothesized by Sprintall at al. (2000). Global HYCOM has a reasonable representation of most of these events. Gordon et al. (2008) also report the annual mean transport increases in each of the three years: -11.2 Sv (2004), -11.7 (2005) and -11.8 (2006) and a similar increasing trend is seen in global HYCOM: -6.8 Sv (2004), -7.0 Sv (2005) and -7.9 Sv (2006), albeit stronger. Thus, the large scale wind forcing across the Pacific and Indian Oceans that drives the ITF variability (Potemra and Schneider, 2007) is simulated well by the NOGAPS forcing product and global HYCOM is responding appropriately.

3.3 Lifamatola Passage

Because of problems with the instruments in the upper part of the mooring and due to blow-over issues, van Aken et al. (2009) were unable to determine transport above 450 m. Below this depth down to ~1250 m, there is weak northward flow into the Maluku Sea and then a reversal to southward flow into the Seram Sea down to the sill (Fig. 3b). The simulated transport between 450-1250 m is not northward, but weakly southward. However, the deep overflow is well represented in global HYCOM with simulated transport (-2.0 Sv) similar to observed transport (-

2.5 Sv) for the flow below 1250m. The observed maximum southward transport is higher in the water column (1588 m) than in HYCOM (1750 m) in part because of inadequate model resolution of the deep channel. Transport is calculated as the vertical integral of the velocity times the width of the channel for a prescribed slab thickness. While both the model and observations indicate the strongest velocities much closer to the respective sill (Fig. 6a), the actual width of the channel decreases more rapidly than can be resolved by HYCOM's vertical grid. Thus the maximum simulated transport is deeper in the water column than the observations suggest. HYCOM indicates relatively strong northward near surface flow (< 450 m) and this will be discussed in more detail later.

The ASV profile comparison (Fig. 6a) is generally very similar but the impact of shallower model topography than observed (Table 1) is seen again in that the simulated overflow is ~200 m shallower than observed. The simulated deep overflow is also stronger and confined to a narrower depth range than the observations. This may be due to the lack of mixing associated with strong tidal forcing at the sill or to an inadequate entrainment parameterization associated with overflows (Xu et al., 2006). van Aken et al. (2009) report regular reversals upwards of ±1 m/s in the deep flow (1500 m) at Lifamatola Passage associated with the tides, but these are absent in HYCOM because this version does not contain tidal forcing. The potential temperature (Fig. 6b) and salinity (Fig. 6c) profiles indicate realistic water mass characteristics at these depths in the passage. The salinity minimum occurs at a similar depth (~800 m), although the model is fresher (34.58 psu) than observed (34.60 psu).

3.4 Lombok Strait

The vertical structure of simulated transport at the three outflow passages also agrees quite well with the INSTANT observations. At Lombok Strait (Fig. 3d), both the observations and model indicate surface trapped flow down to the sill at 300 m. This is also reflected in the mean ASV (Fig. 7a) where the strongest southward flow is western intensified in both the observations (Sprintall et al., 2009 and Hautala et al., 2001) and global HYCOM. The simulated variability (Fig. 7d) is also western intensified, but HYCOM does not reproduce a surface maximum that diminishes with depth.

3.5 Ombai Strait

The profile of simulated transport at Ombai Strait is consistent with the observations (Fig. 3e) except that HYCOM has a weak near surface bias and a strong subsurface bias, while the ASV (Fig. 7b) shows the core of the ITF intensified on the southern side of the strait. The simulated profile of the mean and variability (Fig. 7e) of the southwestward flow is similar to the observations, but HYCOM has a single core at 100 m whereas INSTANT suggests dual cores at the surface and 180 m. The observed subsurface ITF core is found during the northwest monsoon when the flow at the surface is reversed by the local winds (Sprintall et al., 2009, Sprintall et al., 2010). Global HYCOM also simulates the northwest monsoon effect near surface (approximately the top 30-50 m) flow reversal and the subsurface maximum, although it is shallower (150 m) than observed (not shown). Both the observations and model also indicate a deep relative maximum near 900 m associated with the outflow of the Indonesian Intermediate Water (Talley and Sprintall, 2005).

In a new finding reported by Sprintall et al. (2009), the INSTANT moorings indicate weak mean flow away from the Indian Ocean and toward the internal Indonesian Seas on the northern

side of Ombai Strait. They hypothesize these two velocity cores are associated with the South Java Current (SJC) and the South Java Undercurrent (SJUC). There is only a hint of this eastward flow very near the surface in global HYCOM (Fig. 7b) and the absence of the deeper subsurface jet may be due to inadequate model topography on the northern side of the strait or an incorrect sill depth at Sumba Strait that permits flow to enter the Savu Sea. Iskandar et al. (2006) have a clear representation of the SJC and SJUC in the 1/10° OGCM for the Earth Simulator (OFES), but their analysis region ends just west of the Savu Sea and it is unclear from their study if these currents continue all the way to Ombai Strait. At its narrowest, Ombai Strait is only four model gridpoints wide in 1/12° global HYCOM and perhaps horizontal resolution is preventing this counter flow from being properly simulated this far to the east. We thus examine a 1/25° version of global HYCOM that is under development at NRL and is presently being spun-up with ERA40-QuikSCAT scaled climatological forcing (see the end of section 2). That simulation produces weak (less than 10 cm/s) mean eastward flow on the north side of Ombai Strait at 125°E from the surface down to ~550 m and extending southward from the coast of Alor Island a distance similar to what the observations suggest; a near twin climatologically forced 1/12° resolution simulation does not exhibit any mean eastward flow (not shown). This suggests that higher horizontal resolution may be needed to robustly simulate the mean nearshore SJC and SJUC this far east in Ombai Strait. But, 1/25° HYCOM also suggests that this eastward mean flow retroflects and joins the main ITF current traveling to the southwest (Fig. 8) and thus the mean flow does not participate in the formation of Indonesian Throughflow Water, as suggested by Sprintall et al. (2009). As the Nusa Tenggara Current (NTC) (Wijffels et al., 2008) travels eastward along the north side of the Alor Island, it seeks the western-most boundary as it turns southward into Ombai Strait, thus preventing Indian Ocean waters from entering the Banda Sea.

However, this does not preclude the possibility that flow of Indian Ocean origin may enter the southern Banda Sea via Ombai Strait in the form of events (e.g. strong coastally trapped Kelvin waves). Gordon et al. (1994) suggest water of Indian Ocean origin in the southern Banda Sea based on data from a single cruise in December 1991.

3.6 Timor Passage

Similar to Lombok Strait, the flow through Timor Passage is largely surface trapped (Fig. 3f) and the largest difference between observations and model is in the top 100 m slab; otherwise the model has a weak bias for all the depths below. The simulated ASV mean (Fig. 7c) is in close agreement with the observations (Sprintall et al., 2009). In both, the strongest surface flow is centered over the deepest part of the channel and a secondary subsurface southwestward maximum is centered at ~1200 m (also observed by Molcard at al., 1996), and the bottom few hundred meters of the deep channel shows weak northeastward flow from the Indian Ocean toward the Timor Sea. Weak northeastward flow is also found in the model at depths of ~200-500 m on the shelf in the southern side of the passage that is not present in the observations. The simulated ASV variability (Fig. 7f) is highest on the north side of Timor Passage, albeit stronger than observed, and the deep variability maximum is associated with the westward flow, not the eastward flow as the observations indicate.

4. Circulation pathways in 1/12° global HYCOM

Having established that 1/12° global HYCOM has a realistic representation of the circulation through the INSTANT-monitored straits, we focus on the overall simulated circulation patterns across the Indonesian Seas. The simulated total ITF transport is similar to the INSTANT estimates (13.4 vs. 15.0, respectively), but the weak simulated flow through Makassar

Strait (Fig. 2) indicates global HYCOM is incorrectly partitioning the flow through the western and eastern inflow passages. This is perhaps the largest shortcoming of this particular simulation.

4.1 Eastern upper ocean ITF circulation pathways

Global HYCOM simulates -5.2 Sv of total transport through the eastern throughflow route (Fig. 2: Sulawesi – New Guinea section), of which -2.0 Sv is associated with the deep overflow at Lifamatola Passage. The remaining -3.2 Sv is generally surface intensified in the upper 200-300 m (Fig. 3c) and most enters the Indonesian Seas via Halmahera Sea carrying water of South Pacific Ocean origin (Fig. 2: Halmahera – New Guinea section vs. Sulawesi – Halmahera section). Layer four has a depth range of ~20-120 m across most of the Indonesian Seas domain and thus represents upper thermocline waters (Fig. 9a). Some of these near surface waters entering via the Halmahera Sea turn northward through the various passages into the Maluku Sea (1.4 Sv in the top four layers) and eventually join the North Equatorial Countercurrent (NECC). However, 1.0 Sv (top four layers) of upper thermocline waters enter the northern Banda Sea. This is counter to Gordon (2005) who uses salinity within the thermocline to identify ITF source regions. He indicates that saltier South Pacific subtropical water does not spread significantly into the Banda Sea via the Halmahera Sea at these depths (his Fig. 3d). While a detailed water mass analysis is beyond the scope of this paper, simulated upper thermocline salinity in the northern Banda Sea does show the influence of South Pacific waters (not shown).

Below layer four lies a concentration of layers that represent the thermocline in HYCOM. The relatively thin layer 9 is at ~150 m across most of the domain and is near the depth of maximum throughflow (Fig. 9b). In addition to continued inflow toward the interior seas via the Halmahera Sea, this layer also indicates southward flow through the Maluku Sea that is of South

Pacific origin. However, caution must be exercised in interpreting this result. There are a few very thin layers near this depth that indicate southward flow from the Maluku Sea to the Seram Sea, but Fig. 3b clearly indicates net northward flow when multiple, thicker layers higher in the water column are averaged together.

According to Gordon (2005), South Pacific inflow waters enter the interior seas by way of the Halmahera Sea in the lower thermocline over a depth range of ~275-325 m. This is simulated in global HYCOM and northern Banda Sea salinities have a strong South Pacific influence. A southward subsurface maximum in transport is simulated through the Halmahera Sea over this depth range (not shown), but it is appreciably weaker than the unrealistically simulated upper thermocline component (-0.7 Sv vs. -1.9 Sv, respectively).

4.2 Western upper ocean ITF circulation pathways

As discussed earlier, Makassar Strait carries ~75-80% of the total ITF transport and the source region of these inflow waters throughout the thermocline is the North Pacific via the Sulawesi Sea (Gordon, 2005). However, it is presently not known what contribution is coming from the Sulu Sea. Ilahude and Gordon (1996) suggest the presence of Sulu Sea water in Makassar Strait during the northwest monsoon season, but it is not quantified. Both observations and models (Han et al., 2009 among others) indicate net flow from the western Pacific Ocean through the South China Sea (SCS) or via the internal Philippines Seas. This flow then enters the Sulu Sea and exits through Sibutu Passage. In simulations with Sibutu Passage opened and completely closed, Metzger and Hurlburt (1996) note no change in transport for both Makassar Strait and the Pacific to Indian Ocean Throughflow (their experiments 7 and 8).

Global HYCOM has nearly equal transports from Sibutu Passage and the eastern Sulawesi Sea (mainly from the Mindanao Current) feeding into Makassar Strait (Fig. 2). In the net the simulated upper thermocline waters come from the Sulu Sea (Fig. 9a), whereas the mid-thermocline waters (and below) enter through the eastern Sulawesi sea (Fig. 9b). While there are no observational estimates of Sibutu Passage transport, the simulated value appears unrealistically high in relation to the flow entering the Sulawesi Sea from the North Pacific. Most of the simulated flow in the upper five layers through Sibutu Passage turns eastward and joins the NECC (2.3 Sv) rather than travel southward to Makassar Strait (0.8 Sv). Below layer five, an additional 0.5 Sv enters Makassar Strait from Sibutu Passage (total 1.3 Sv) but the remaining 6.0 Sv enters from the Sulawesi Sea. This near surface eastward turning agrees with the results from a linear model with a Sverdrup (1947) interior, Munk (1950) western boundary layers and is consistent with the theory of Godfrey (1989) for including islands. In particular, the 1/16° global barotropic linear numerical model using the same ERA15 forcing indicates that the waters from the Sulu Sea exit at Sibutu Passage and all turn eastward to join the NECC, suggesting that the near surface flow is quasi-linear.

There is modeling evidence that suggests the upper ocean flow through the Sulawesi Sea may be dependent on the larger scale wind forcing. The main difference in a second 1/12° global HYCOM simulation is the spin up, which used ERA40-QuikSCAT scaled climatological forcing. That simulation was then extended interannually using the same model topography and using the same NOGAPS forcing as in the main experiment, but with QuikSCAT scaling also applied to the wind speeds. This second simulation exhibits a direct connection of North Pacific waters entering into the northern Sulawesi Sea from the Mindanao Current in the top five layers and directly participating in the upper ocean Makassar Strait throughflow (not shown), which is

opposite to the main experiment analyzed in this paper. However, the ratio of southward transport through Sibutu Passage and westward transport through the Sulawesi Sea in the second simulation is similar to the primary experiment presented here.

The topography and sill depth in Sibutu Passage are not accurately known since there are significant differences among the various digital databases. Some suggest a sill on the order of 200-250 m and the model sill is 269 m using the NRL DBDB2 database. As noted earlier, we have subsequently modified the 1/12° global HYCOM topography in the key Indonesian passages using Smith and Sandwell (1997). This resulted in an overall shallowing of Sibutu Passage model topography, especially in the passages on the western side of the strait, and the new sill depth is 241 m. In another supplementary simulation using ERA40-QuikSCAT climatological forcing and this modified topography (among other model changes), the transport through Sibutu Passage drops to -2.2 Sv with an appreciable reduction of flow on the western side of the passage. While still contributing to the Makassar Strait throughflow, the influence of waters from the Sulu Sea is reduced and once again this highlights the crucial role of topography in the Indonesian Seas. Along with accuracy of the atmospheric forcing, accurate knowledge of the bottom depths may be a limiting factor in simulation skill in this region.

The southward flow through Makassar Strait encounters the Dewakang Sill (~680 m) which is the controlling depth for the circulation through the western ITF route (Gordon et al., 2003). As simulated in global HYCOM, this submerged multi-passage plateau causes the flow to separate into three branches, an eastern and central branch that feeds the eastward flowing NTC and a western branch that directly feeds Lombok Strait (Fig. 10). At depths above the controlling sill at Lombok Strait (~300 m), the western branch is the strongest of the three and a portion also turns eastward as it encounters the Nusa Tenggara archipelago. With increasing depth the central

branch is the first to be totally blocked by the topography and still deeper the western and eastern branches have approximately the same speed before also being totally blocked by the sill (not shown).

4.3 Deep ocean ITF circulation pathways

Global HYCOM has a good representation of the water mass properties and velocity of the deep overflow at Lifamatola Passage (Fig. 6) and the strongest overflow is concentrated in layers 20-23 (approximate layer depths from 1350-1700 m) with transports of -0.48, -0.46, -0.88 and -0.21 Sv, respectively. In the deep ocean, the flow will travel along isopycnals and this is an advantage of using global HYCOM. The origins of the simulated Lifamatola overflow reveal both North Equatorial Current (NEC) and South Equatorial Current (SEC) components that exhibit a strong seasonal variation. The JFM average of these layers indicates the source waters are exclusively from the NEC, which is true for both the 4-layer average (Fig. 11a) and the individual layers themselves (not shown). The westward flowing branch bifurcates at the Sangihe Ridge (3°N), which separates the deep Pacific Ocean from the Sulawesi Sea (Fig. 1). One branch turns southward into the Maluku Sea and flows within the western boundary of a recirculation gyre that fills the basin before it continues through Lifamatola Passage. The JAS average of these layers (Fig. 11b) indicates the flow is exclusively of SEC origin flowing northwestward along the New Guinea coast and then into the Maluku Sea. This is consistent with O'Driscoll and Kamenkovich (2009) that examined the source of Lifamatola overflow in the Princeton Ocean Model using output from August (but they did not look at the opposite season). The bifurcation latitude along the Sangihe Ridge has shifted northward to 5.5°N with a second branch turning westward into the region just north of the Halmahera Islands. The southward flow

along the ridge and within the recirculation gyre in the southern Maluku Sea is stronger in this season by about 2 cm/s.

Both the observations and the model indicate deep flow from the Indian Ocean toward the interior seas at Timor Passage (Fig. 7c). The simulated deep transport, calculated along a line near where the INSTANT moorings were located, is very weak: layer 21 = 0.03 Sv and layer 22 = 0.01 Sv. These two layers are isolated from the interior seas since they are deeper than the sill depths to the east of Timor Island and along the Outer Banda Arc. Thus, their salinity signature is of Indian Ocean origin and in the mean these waters do not participate in the deep water formation processes of the Banda Sea in global HYCOM results. The net eastward flow into these isolated layers implies weak diapycnal upwelling across the isopycnal layer interfaces. Both the observations and model show a velocity variability maximum in the deep part of the trench (Fig. 7f). This suggests that diapycnal mixing or events might allow Indian Ocean waters to spill into the Banda Sea. However, simulated salinity within these layers indicates two distinct water masses on either side of Leti Strait (not shown).

5. Filling in the INSTANT network gaps with global HYCOM

5.1 Inflow through the Java and Arafura Seas

The INSTANT-monitored estimates of transport through the straits at Makassar, Lombok, Ombai and Timor are representative of the total flow (except perhaps for the very near surface flow <25 m), but at Lifamatola Passage various issues prevented the calculation of transport in the upper 450 m of the water column. van Aken et al. (2009) also indicate that it is questionable to compute transport above 1250 m from a single mooring due to the increasing width of the strait. Assuming there is negligible upper ocean flow at Lifamatola Passage, the sum of the two

inflow straits (-14.1 Sv) is almost one Sverdrup smaller than the sum of the three outflow straits (-15.0 Sv). Where might this missing inflow come from? Global HYCOM suggests it can approximately be made up by adding the inflow through Karimata Strait (-0.6 Sv) in the Java Sea and Torres Strait (-0.2 Sv) in the Arafura Sea (Fig. 2). The simulated flow through these straits exhibits a clear annual cycle in response to the monsoonal forcing, but they are ~180° out of phase with each other. Karimata Strait produces the largest inflow (outflow) during the northwest (southeast) monsoon while the cycle is reversed at Torres Strait. The South China Sea-Indonesian Seas Transport Exchange (SITE) program is an on-going field experiment between the First Institute of Oceanography (China), the Agency for Marine and Fishery Research (Indonesia) and Lamont-Doherty Earth Observatory (Columbia University, USA) that may soon provide some of the first observational estimates of Karimata Strait transport and thus provide a volume transport estimate at one of the missing inflow straits. While not contemporaneous with the INSTANT program, it will give guidance on the performance of global HYCOM and other models in the shallow Java Sea.

Qu et al. (2005, 2009) refer to the flow through Karimata Strait as being one component of the South China Sea Throughflow (SCSTF). They hypothesize that this branch of the SCSTF inhibits near surface water of Pacific Ocean origin from flowing southward in Makassar Strait, thus creating the thermocline velocity maximum in that strait (Fig. 4). Further, Tozuka et al. (2009) use 0.4° MOM3 and indicate the Makassar Strait subsurface velocity maximum is simulated when Karimata Strait is opened (with a transport of -1.6 Sv), but not when it is closed. Their model simulates northward flow in the top 50 m at Makassar Strait from approximately November through February. Gordon et al. (2008) (their Fig. 2) show the velocity profile at Makassar Strait over the INSTANT time frame, but they exclude the top 25 m of the water

column. While there are reductions in the southward flow, there are no flow reversals measured from the moorings. Fang et al. (2009) use the slightly finer resolution 1/6° MOM2 that simulates -1.2 Sv at Karimata Strait, which is the same value obtained in 0.1° OFES (Tozuka et al., 2009). Lastly, Yaremchuk et al. (2009) use an inverse modeling approach to estimate SCSTF that "best fits" the climatological T and S fields within the SCS and they obtain a Karimata Strait transport of -0.3 Sv. They note that a possible reason for the wide range in simulated values of the SCSTF among various models may be due to the representation of the shallow topography and how it is discretized in the vertical. In the OGCM examples cited above, Karimata Strait transport is successively smaller with increased horizontal resolution among the models and 1/12° global HYCOM falls at the low end of the range (-0.6 Sv).

The topography used in global HYCOM is typically shallower than observed, but Table 1 indicates that Torres Strait is the exception. Wolanski et al. (1988) indicate strong tidal currents but essentially no net exchange through this strait due to the numerous reefs, whereas the deeper model sills are allowing a small amount (-0.2 Sv) to contribute to the ITF.

5.2 Outflow along the Nusa Tenggara archipelago

Lombok Strait, Ombai Strait and Timor Passage are clearly the major outflow ports, but what about the other minor passages along the archipelago that separates the Indonesian Seas from the Indian Ocean. Are any of these straits important with regard to the total ITF? Hautala et al. (2001) and Wijffels et al. (2008) suggest they are dominated by tidal and frictional forces and do not play a major role. While this version of HYCOM does not include tidal forcing, we can nonetheless quantify the transport through four straits that are resolved on the model grid but excluded from the INSTANT network (Table 2). As noted earlier, the coastlines and widths are

fairly well defined but the depths within the model straits are generally too shallow because of the spatial smoothing and this will bias the simulated transport on the low side. Of these four additional straits, Sape Strait carries the largest transport (-0.24 Sv) and in fact is larger than the flow through the very wide but shallow Torres Strait (-0.17 Sv). Haultala et al. (2001) indicates Sape Strait is ~19 km wide with a sill depth of < 200 m. Additionally, two short shipboard ADCP surveys were performed in December 1995 (9 hour duration) and March 1998 (13.2 hour duration) that produced transport in the upper 150 m of 1.4±0.4 Sv and -0.2±0.1 Sv, respectively. The 1995 cruise indicates this strait can carry a considerable amount of transport (albeit, in this case toward the Flores Sea), but the short nature of the cruises prevents us from learning much about the mean magnitude and direction of the flow. However, all together these four "missing" straits only account for -0.37 Sv in global HYCOM, or less than 3% of the total Indonesian throughflow. Thus their exclusion is well within the error bars of the total transport estimates.

5.3 Outflow on the shelf south of the main Timor Passage channel

Another potential gap in the INSTANT network is the large shallow continental shelf area to the south of the Timor Passage instruments. Cresswell et al. (1993) indicates the transport over the shelf is generally less than 1 Sv and concludes the shelf does not significantly contribute to the overall throughflow. Using this knowledge, Sprintall et al. (2009) describe their reasoning for the placement of the mooring deployments and believe they are fully measuring the transport through Timor Passage. In this case an advantage of a numerical ocean model is that the transport through the passage can be calculated across varying widths and global HYCOM corroborates that the flow over the Australian shelf is indeed very small. The simulated transport value depicted in Fig. 2 is -5.9 Sv for a section that traverses the passage from land-to-land, i.e. Timor Island in the north to the Australian mainland in the south. Along this same section,

HYCOM was also sampled using only those model gridpoints with topographic depths greater than 100 m and then those greater than 200 m. The simulated transport is -6.1 Sv and -6.0 Sv, respectively. (The former section contained four more model gridpoints than the latter section.) The transport is actually smaller when using the full land-to-land section because HYCOM indicates weak eastward flow over the shelf region (Fig. 12). Nonetheless, no matter how it is computed the total transport only differs by a few tenths of a Sverdrup and the model confirms that the Timor Passage transport is accurately measured by the INSTANT moorings.

6. Discussion and summary

The multi-national INSTANT field program was designed and implemented to provide the first long-term (2004-2006) contemporaneous and comprehensive view of the Indonesian Throughflow (ITF). It has successfully furnished an important new benchmark for both the observational and numerical modeling communities. Given this expanded knowledge base, we make one of the first model-data comparisons with an eddy-resolving global ocean model. Additionally, we use the simulated output to complement the INSTANT observations and provide a more complete depiction of the circulation within the Indonesian Seas.

A comparison between the best observation-based estimate of total volume transport at the INSTANT outflow passages (-15.0 Sv) and transport from 1/12° global HYCOM (-13.4 Sv) indicates that the simulated mean ITF transport falls within the range of the INSTANT observational estimates (-10.7 to -18.7 Sv). The two main contributors to the throughflow are wind forcing (estimated from Sverdrup flow) and the upper ocean flow of the global thermohaline circulation. Impediments within the Indonesian Seas that may reduce the throughflow transport include form drag (i.e. pressure gradient blocking), bottom friction and

increased vertical mixing. The simulated ITF transport in HYCOM is similar to the lowest-order Sverdrup transport (-14.3 Sv) determined by a 1/16° linear model (described in section 4.2) using the same ERA15 forcing. Additionally, Sprintall et al. (2009) notes the ITF transport predicted from mean scatterometer wind stresses using the Godfrey (1989) Island Rule over the INSTANT period is -13.1 to -13.5 Sv. This would suggest that the ITF is essentially a wind driven flow. However, an examination of contributions to the Indo-Pacific component of the meridional overturning circulation (MOC) transport indicates the throughflow in global HYCOM includes a -3.7 Sv contribution from the global MOC, i.e. the part of the basin-wide northward abyssal transport in the South Pacific that is not compensated by overlying southward transport.. The simulated value is similar to previous studies (Schmitz, 1995 [-4.0 Sv]; Shriver and Hurlburt, 1997 [-5.7 Sv]; Goodman, 1998 [-2.0 Sv]; Speich and Blanke, 2001 [-5.3 Sv]). Together, the Sverdrup transport (-14.3 Sv) and the MOC (-3.7 Sv) predict an ITF transport of at least -18.0 Sv versus -13.4 Sv in global HYCOM, indicating that the impeding forces in the model are reducing the ITF transport of this prediction by at least 25%.

Shriver and Hurlburt (1997) offer a three-level schematic (their Plate 4) of the pathways feeding the ITF based on a 6-layer 0.5° Navy Layered Ocean Model (NLOM) simulation forced by Hellerman and Rosenstein (1983) winds and the pathways simulated by global HYCOM are similar. In HYCOM, the southern hemisphere connection to the northern hemisphere is fed by two main pathways: 1) currents along the north coast of New Guinea retroflecting into the NECC east of Halmahera Island and 2) via Equatorial Undercurrent (EUC) upwelling into the surface layers. This northern hemisphere connection to the ITF via Makassar Strait is through Sibutu Passage in the top six layers but through the Sulawesi Sea in layers 7-15 (i.e. down to the Dewakang sill) as noted in Section 4.2.

In the surface layers (1-7) the pathways feeding the ITF are complex and generally enter the Indonesian Seas after a circuitous journey through the northern hemisphere as described above. A notable difference in HYCOM is that the ERA15 winds produce a strong South Equatorial Countercurrent. Thus there is no direct connection of SEC waters to the northern hemisphere in the surface layers that was simulated by NLOM. In the upper EUC layers (8-11), a direct SEC connection to the throughflow is established via flow along the north coast of New Guinea that enters the Indonesian seas east of Sulawesi. In the lower EUC layers (11-13), most of the SEC retroflects and turns back into the EUC where it eventually upwells in the eastern Pacific, mainly into the top four layers. In the top three layers the upwelled water takes a broad interior route into both the northern and southern hemispheres, while in layer 4 it enters the northern hemisphere via the SEC and retroflects into the NECC east of Halmahera Island. Below layer 5 the SEC is no longer fed by upwelled water from the EUC and the SEC carries nearly all of the water from the southern to northern hemisphere, with most retroflecting into the NECC east of Halmahera Island. In the layers below the Makassar Strait sill down to the governing ITF sill (16-19), the southern and northern hemisphere connection is through the Maluku Sea via Lifamatola Passage. In NLOM this deep flow entered via Makassar Strait because the bottom topography was confined to the abyssal layer in that model.

The transport pathways are also reasonably distributed among the Indonesian Seas straits (Fig. 2). The largest discrepancy is noted at the western inflow where the Makassar Strait simulated transport accounts for only 54% of the total ITF, rather than the observed 77%. The downstream model topography at Dewakang Sill is 195 m too shallow and simulated transport is significantly weaker than observed over this depth range (Fig. 3a), suggesting that inaccurate model topography is the main cause for the low simulated transport. Supplementary 1/12° global

HYCOM simulations with identical climatological ERA40-QuikSCAT forcing using the same topography as the main experiment and a second simulation using a modified topography to more accurately reflect the sill depth in all the key passages indicate the ratio of Makassar Strait transport to total ITF transport increases from 60% to 67%, respectively. Global HYCOM is able to simulate the thermocline maximum of along strait velocity at Makassar Strait, albeit deeper than observed (Fig. 4), the deep overflow at Lifamatola Passage (Figs. 2 and 3b), and the observed surface intensification at the three outflow passages Lombok Strait, Ombai Strait and Timor Passage (Figs. 3d-f and 7).

Sprintall et al. (2009) report that the INSTANT moorings indicate weak mean flow from the Indian Ocean toward the Indonesian Seas on the north side of Ombai Strait (Fig. 7b). They hypothesize these two velocity cores are associated with the South Java Current and South Java Undercurrent but there is only a hint of the near-surface current in the 1/12° HYCOM simulation. We looked at the impact of horizontal resolution on the formation of these currents by examining a 1/25° version of global HYCOM using climatological forcing. The higher resolution model produces eastward flow (< 10 cm/s) on the north side of Ombai Strait at the same location as the mooring with speeds comparable to the observations. This suggests that higher horizontal resolution may be needed to robustly simulate these currents this far east in Ombai Strait. In the mean this current retroflects into the main ITF current and does not enter the Banda Sea.

Perhaps the largest shortcoming of the main global HYCOM simulation is the incorrect partitioning of ITF inflow between the western and eastern passages in the upper ocean. A substantial amount (-3.2 Sv) of generally surface intensified simulated transport enters the Banda Sea via the Halmahera Sea and is of South Pacific Ocean origin. This is counter to Gordon (2005) that indicates only lower thermocline (not upper to mid-thermocline) waters enter via this

route with the high salinity signature of the South Pacific. Through the western passages, the model produces a relatively large amount of southward transport (-3.6 Sv) through the Sulu Sea via Sibutu Passage. However, much of the flow in the upper five layers turns eastward into the Sulawesi Sea rather than traveling southward down Makassar Strait, another contributing factor to the smaller than observed transport. There is modeling evidence to suggest that the upper ocean flow through the Sulawesi Sea is dependent on the large scale wind forcing. A supplementary 1/12° global HYCOM simulation was spun-up with ERA40 forcing and then extended interannually over the INSTANT time frame with NOGAPS forcing, both with the wind speeds scaled to QuikSCAT scatterometer wind speeds. This simulation exhibits a direct connection of North Pacific waters entering the Sulawesi Sea in the top five model layers and directly participating in the upper ocean Makassar Strait throughflow, consistent with the results of Sverdrup flow from linear simulations.

The main deep ITF circulation pathway is through the Maluku Sea, via Lifamatola Passage and into the Seram/Banda Seas. Tracing the origins of this simulated deep overflow reveals both NEC and SEC components that exhibits strong seasonal variations. Global HYCOM indicates the overflow is of NEC origin in boreal winter-spring (Fig. 11a), whereas it is of SEC origin in the summer-autumn (Fig. 11b).

We also used global HYCOM to fill in the gaps of the INSTANT network and corroborate that the program has adequately measured the total ITF transport. Makassar Strait carries the majority of the inflow ITF transport, but how much enters through the wide and shallow Java and Arafura Seas? The model suggests -0.6 Sv and -0.2 Sv (respectively), or ~6% of the total. There are also some minor passages in the Nusa Tenggara archipelago that separates the Indonesian Seas from the Indian Ocean, but the sum of all “missing” minor straits accounts for

less than 3% of the total throughflow. Finally, the simulated transport across Timor Passage has been calculated using varying width sections to include or exclude the shallow shelf area to the south of the main channel, and global HYCOM corroborates the work of Cresswell et al. (1993) that indicates negligible throughflow over the shelf (Fig. 12).

The baseline model-data comparisons presented in this manuscript indicate that overall, 1/12° global HYCOM has a realistic representation of the Indonesian Throughflow and can be used to study the circulation pathways. There are issues that need to be addressed such as the incorrect partitioning of inflow between the western and eastern routes and the excessive upper thermocline influx of South Pacific origin waters via the Halmahera Sea. Some of the problems may be corrected by more accurate model topography, but there can be large discrepancies at the key passages among the various digital topographic databases so it is difficult to know what the truth is. Thus, accurate knowledge of the topography (and appropriate interpolation to the model grid) will be one limiting factor in simulation skill for some time to come. Another factor controlling the partitioning is the atmospheric forcing and we have discussed the sensitivity of the circulation pathways to different products. Equally important have been upgrades to the model physics since these simulations were integrated. Presently, 1/12° and 1/25° global HYCOM simulations with improved topography and physics are underway using climatological forcing and these are being extended with interannual forcing that spans the INSTANT time frame. Preliminary analysis indicates improved portioning between the western and eastern routes and ITF total transport that is now larger than the INSTANT estimates. The incorporation of tides (Arbic et al., 2010) and their impact on the throughflow transport and vertical structure of the water column is also under further investigation.

Acknowledgements

The modeling component of this article is a contribution from the "6.1 Dynamics of the Indonesian Throughflow (ITF) and Its Remote Impact" project sponsored by the Office of Naval Research under program element number 61153N. Grants of computer time were provided by the Department of Defense (DoD) High Performance Computing Modernization Program and the simulations were performed on the IBM Power 4+ (Kraken), the IBM Power 6 (daVinci) and the Cray XT5 (Einstein) at the Navy DoD Supercomputing Resources Center, Stennis Space Center, MS. The INSTANT component of this article was sponsored by National Science Foundation grants OCE-07-25935 (Lamont-Doherty Earth Observatory [LDEO]) and OCE-07-25476 (Scripps Institution of Oceanography [SIO]). We also thank Dr. Alan Wallcraft for his computer expertise and developmental work on HYCOM. This is NRL contribution NRL/JA/7320--09-9336 and LDEO contribution 7346. It has been approved for public release and distribution is unlimited.

Table 1: Sill depths (in meters) of the key straits and passages in the Indonesian Seas from the scientific literature and those used in 1/12° global HYCOM. See Fig. 1 for the geographical location. The overall sill depth for the Indonesian Throughflow is at Leti Strait. The governing sills at the north end of Maluku Sea are deeper than those at the southern end (Lifamatola Passage).

Strait or Passage	Observed estimate	1/12° global HYCOM
Inflow Passages		
Sangihe Ridge (divides Pacific Ocean and Sulawesi Sea)	1350[a]	1227
Makassar Strait (Dewakang Sill)	680[a]	485
Halmahera Sea passages	580[a]	485
Lifamatola Passage	1940[b]	1777
Karimata Strait (South China Sea – Java Sea connection)	-	29
Torres Strait (Arafura Sea)	< 10[c]	23
Outflow Passages		
Lombok Strait	300[a]	263
Strait between Alor and Atauro Islands (upstream of Ombai Strait)	1450[d]	1701
Wetar Strait (upstream of Ombai Strait)	2450[d]	2318
Timor Passage (southern end)	1890[e]	1467
Leti Strait (north end of Timor Island)	1250[e]	1152
Sumba Strait (north of Sumba Island)	900[e]	573
Savu Strait (connection between Savu Sea and Indian Ocean)	1150[e]	1016
Outer Banda Arc	1250[f]	993

Sources for sill depths: [a]Gordon et al. (2003), [b]van Aken et al. (1988), [c]Wolanski et al. (1988), [f]Sprintall et al. (2010), [e]Sprintall et al. (2009), [f]INSTANT web page (http://www.marine.csiro.au/~cow074).

Table 2: Mean 2004-2006 transport (Sv) in 1/12° global HYCOM through the straits in the archipelago that separates the Indonesian Seas from the Indian Ocean that are not part of the INSTANT network. Some straits are outside the geographic domain depicted in Fig. 1.

Strait	Approximate longitude, latitude	Geographic location	Model sill depth (m)	Transport (Sv)
Malacca	102°E, 2°N	Connection between the South China Sea and Andaman Sea	20	-0.08
Sunda	106°E, 6°S	Southwest corner of the Java Sea	10[a]	-0.03
Alas	117°E, 9°S	Just east of Lombok Strait	10[a]	-0.02
Sape	119°E, 9°S	Between Alas and Ombai Straits	86	-0.24

[a]The shallowest depth used in the model is 10 m.

References

Arbic, B.K., Wallcraft, A.J., Metzger, E.J., 2010. Concurrent simulation of the eddying general circulation and tides in a global ocean model. Ocean Model. 32:175-187, doi:10.1016/j.ocemod.2010.01.007.

Barron, C. N., Smedstad, L.F., 2002. Global river inflow within the Navy Coastal Ocean Model. Proc. Oceans 2002 MTS/IEEE Conference, Biloxi, Mississippi, USA, pp. 1472–1479.

Bleck, R., 2002. An oceanic general circulation model framed in hybrid isopycnic-Cartesian coordinates. Ocean Model., 4:55-88.

Canuto, V. M., Howard, A., Cheng, Y., Dubovikov, M.S., 2001. Ocean turbulence. Part I: One-point closure model. Momentum and heat vertical diffusivities. J. Phys. Oceanogr., 31:1413-1426.

Canuto, V. M., Howard, A., Cheng, Y., Dubovikov, M.S., 2002. Ocean turbulence. Part II: Vertical diffusivities of momentum, heat, salt, mass, and passive scalars. J. Phys. Oceanogr., 32:240-264.

Carnes, M.R., 2009. Description and evaluation and GDEM-V3.0. NRL Memorandum Rpt., NRL/MR/7330—09-9165.

Chassignet, E.P., Smith, L.T., Halliwell G.R., Bleck, R., 2003. North Atlantic simulations with the HYbrid Coordinate Ocean Model (HYCOM): Impact of the vertical coordinate choice, reference pressure, and thermobaricity. J. Phys. Oceanogr., 33(12):2504-2526.

Cresswell, G.A., Frische, A., Peterson,J., Quadfasel, D.,1993. Circulation in the Timor Sea. J. Geophys. Res., 98(C8):14379-14389.

Fang, G., Wang, Y., Wei, Z., Fang, Y., Qiao, F., Hu, X., 2009. Interocean circulation and heat and freshwater budgets of the South China Sea based on a numerical model. Dyn. Atmos. Oceans, 47:55-72, doi:10.1016/j.dynatmoce.2008.09.003.

Ffield, A., Gordon, A.L., 1996. Tidal mixing signatures in the Indonesian Seas. J. Phys. Oceanogr., 26:1924-1937.

Gibson, J.K., Kallberg, P., Uppala, S., Hernandez, A., Nomura, A., Serrano, E., 1999. ERA ECMWF Re-Analysis Project Report Series: 1. ERA-15 Description (Version 2 – January 1999). European Centre for Medium-Range Weather Forecasts, Reading, Berkshire, UK.

Godfrey, J.S., 1989. A Sverdrup model of the depth-integrated flow for the world ocean allowing for island circulations. Geophys. Astrophys. Fluid Dyn. 45(1–2):89–112.

Goodman, P.J., 1998. The role of North Atlantic deep water formation in an OGCM's ventilation and thermohaline circulation. J. Phys. Oceanogr., 28:1759-1785.

Gordon, A.L., 2005. Oceanography of the Indonesian Seas and their throughflow. Oceanography, 18(4):14-27.

Gordon, A.L., Ffield, A., Ilahude, A.G., 1994. Thermocline of the Flores and Banda Seas. J. Geophys. Res., 99(C9):18235-18242.

Gordon, A.L., Giulivi, C.F., Ilahude, A.G., 2003. Deep topographic barriers within the Indonesian seas. Deep-Sea Res. II, 50:2205-2228, doi:10.1016/S0967-0645(03)00053-5.

Gordon, A.L., Sprintall, J., van Aken, H.M., Susanto, R.D., Wijffels, S., Molcard, R., Ffield, A., Pranowo, W., Wirasantosa, S., 2010. The Indonesian Throughflow during 2004-2006 as observed by the INSTANT program. Dyn. Atmos. Oceans, (this issue).

Gordon, A.L., Susanto, R.D., Ffield, A., Huber, B.A., Pranowo, W., Wirasantosa, S., 2008. Makassar Strait throughflow, 2004 to 2006. Geophys. Res. Lett., 35:L24605, doi:10.1029/2008GL036372.

Halliwell, G. R., 2004. Evaluation of vertical coordinate and vertical mixing algorithms in the HYbrid Coordinate Ocean Model (HYCOM), Ocean. Model., 7(3–4):285–322.

Han, W., Moore, A.M., Levin, J., Zhang, B., Arango, H.G., Curchitser, E., Di Lorenzo, E., Gordon, A., Lin, J., 2009. Seasonal surface ocean circulation and dynamics in the Philippine Archipelago region during 2004-2008. Dyn. Atmos. Oceans, 47:114-137, doi:10.1016/j.dynatmoce.2008.10.007.

Hautala, S.L., Sprintall, J., Potemra, J.T., Ilahude, A.G., Chong, J.C., Pandoe, W., Bray, N., 2001. Velocity structure and transport of the Indonesian Throughflow in the major straits restricting flow into the Indian Ocean. J. Geophys. Res., 106:19,527-19,546.

Hellerman, S., Rosenstein, M., 1983. Normal monthly wind stress over the World Ocean with error estimates. J. Phys. Oceanogr., 13:1093-1104.

Ilahude, A.G., Gordon, A.L., 1996. Thermocline stratification within the Indonesian Seas. J. Geophys. Res., 101(C5):12401-12409.

Iskandar, I., Tozuka, T., Sasaki, H., Masumoto, Y., Yamagata, T., 2006. Intraseasonal variations of surface and subsurface currents off Java as simulated in a high-resolution ocean general circulation model, J. Geophys. Res., 111:C12015, doi:10.1029/2006JC003486.

Kallberg, P., Simmons, A., Uppala, S., Fuentes, M., 2004. ERA-40 Project Report Series: 17. The ERA-40 archive. ECMWF, Reading, Berkshire, UK.

Kara, A.B., Hurlburt, H.E., Wallcraft, A.J., 2005. Stability-dependent exchange coefficients for air-sea fluxes. J. Atmos. Oceanic. Technol., 22:1080-1094.

Kara, A.B., Wallcraft, A.J., Martin, P.J., Pauley, R.L., 2009. Optimizing surface winds using QuikSCAT measurements in the Mediterranean Sea during 2000–2006, J. Mar. Syst., doi:10.1016/j.jmarsys.2009.01.020.

Ko, D.-S., 2002. NRL DBDB2 global 2-minute topography. http://www7320.nrlssc.navy.mil/DBDB2_WWW.

Koch-Larrouy, A., Madec, G., Bouruet-Aubertot, P., Gerkema, T., Bessières, L., Molcard, R., 2007. On the transformation of Pacific water into Indonesian Throughflow water by internal tidal mixing. Geophys. Res. Lett., 34, L04604, doi:10.1029/2006GL028405.

Lee, H.-C., Rosati, A., Spelman, M.J., 2006. Barotropic tidal mixing effects in a coupled climate model: Oceanic conditions in the Northern Atlantic. Ocean Model., 11:464-477, doi:10.1016/j.ocemod.2005.03.003.

Metzger, E.J., Hurlburt, H.E., 1996. Coupled dynamics of the South China Sea, the Sulu Sea, and the Pacific Ocean. J. Geophys. Res., 101(C5):12331-12352.

Meyers, G., 1996. Variation of Indonesian throughflow and the El Niño-Southern Oscillation. J. Geophys. Res., 101(C5):12255-12263.

Molcard, R.M., Ilahude, A.G., Fieux, M., Swallow, J.C., Banjarnahor, J., 1994. Low frequency variability of the currents in the Indonesian Channels (Savu-Roti M1 and Roti-Ashmore Reef M2). Deep Sea Res., 41:1643-1662.

Molcard, R.M., Fieux, M., Ilahude, A.G., 1996. The Indo-Pacific throughflow in Timor Passage. J. Geophys. Res., 101:12411-12420.

Molcard, R., Fieux, M., Syamsudin, F., 2001. The throughflow within Ombai Strait. Deep Sea Res., 48:1237-1253.

Munk,W.H., 1950. On the wind-driven ocean circulation. J. Met. 7 (2):79–93.

Murray, S.P., Arief, D., 1988. Throughflow into the Indian Ocean through Lombok Strait, January 1985-January 1986. Nature, 333:444-447.

O'Driscoll, K.T.A., Kamenkovich, V., 2009. Dynamics of the Indonesian Seas circulation. Part I – The influence of bottom topography on temperature and salinity distributions. J. Mar. Sys., 67:119-157.

Potemra, J.T., 2005. Indonesian throughflow transport variability estimated from satellite altimetry. Oceanogr., 18:94-103.

Potemra, J.T., Schneider, N., 2007. Interannual variations of the Indonesian throughflow. J. Geophys. Res., 112:C05035, doi:10.1029/2006JC003808.

Qu, T., Du, Y., Meyers, G., Ishida, A., Wang, D., 2005. Connecting the tropical Pacific with the Indian Ocean through South China Sea. Geophys. Res. Lett., 32:L24609, doi:10.1029/2005GL024698.

Qu, T., Song, Y.T., Yamagata, T., 2009. An introduction to the South China Sea throughflow: Its dynamics, variability, and application for climate. Dyn. Atmos. Oceans, 47:3-14, doi:10.1016/j.dynatmoce.2008.05.001.

Robertson, R., Ffield, A., 2005. M_2 baroclinic tides in the Indonesian Seas. Oceanography, 18(4):62-73.

Rosmond, T.E., Teixeira, J., Peng, M., Hogan, T.F., Pauley, R., 2002. Navy Operational Global Atmospheric Prediction System (NOGAPS): Forcing for ocean models. Oceanography, 15(1):99-108.

Schiller, A., 2004. Effects of explicit tidal forcing in an OGCM on the water-mass structure and circulation in the Indonesian throughflow region. Ocean Modell., 6:31-49.

Schiller, A., Fiedler, R., 2007. Explicit tidal forcing in an ocean general circulation model. Geophys. Res. Lett., 34:L03611, doi:10.1029/2006GL028363.

Schmitz, W.J., Jr., 1995. On the interbasin-scale thermohaline circulation. Rev. Geophys., 33:151-173.

Shriver, J.F., Hurlburt, H.E., 1997. The contribution of the global thermohaline circulation to the Pacific to Indian Ocean throughflow via Indonesia. J. Geophys. Res., 102(C3):5491-5511.

Smith, W. H. F., Sandwell, D.T., 1997. Global seafloor topography from satellite altimetry and ship depth soundings. Science, 277:1957-1962.

Speich, S., Blanke, B., 2001. Warm and cold water routes of an O.G.C.M. thermohaline Conveyor Belt. Geophys. Res. Lett., 28(2):311-314.

Sprintall, J., Gordon, A.L., Murtugudde, R., Susanto, R.D., 2000. A semiannual Indian Ocean forced Kelvin wave observed in the Indonesian Seas in May 1997. J. Geophys. Res., 105(C7):17217-17230.

Sprintall, J., Wijffels, S.E., Gordon, A.L., Ffield, A., Molcard, R., Susanto, R.D., Soesilo, I., Sopaheluwakan, J., Surachman, Y., van Aken, H.M., 2004. INSTANT: A new international array to measure the Indonesian throughflow. EOS, 85(39), 28 September 2004, 369, 376.

Sprintall, J., Wijffels, S.E., Molcard, R., Jaya, I., 2009. INSTANT: Direct estimates of the Indonesian throughflow entering the Indian Ocean: 2004-2006. J. Geophys. Res., 114:C07001, doi:10.1029/2008JC005257.

Sprintall, J., Wijffels, S.E., Molcard, R., Jaya, I., 2010. Direct evidence of the South Java Current system in Ombai Strait. Dyn. Atmos. Oceans, (this issue).

Steele, M., Morley, R., Ermold, W., 2001. PHC: A global ocean hydrography with a high quality Arctic Ocean. J. Climate, 14:2079-2087.

Sverdrup, H.U., 1947. Wind-driven currents in a baroclinic ocean - with application to the equatorial currents of the eastern. Pacific. Proc. Natl. Acad. Sci. U.S.A. 33(11):318–326.

Talley, L.D., Sprintall, J., 2005. Deep expression of the Indonesian Throughflow: Indonesian Intermediate Water in the South Equatorial Current. J. Geophys. Res., 110:C10009, doi:10.1029/2004JC002826.

Tozuka, T., Qu, T., Masumoto, Y., Yamagata, T., 2009. Impacts of the South China Sea Throughflow on seasonal and interannual variations of the Indonesian Throughflow. Dyn. Atmos. Oceans, 47:73-85, doi:10.1016/j.dynatmoce.2008.09.001.

van Aken, H.M., Brodjonegoro, I.S., Jaya, I., 2009. The deepwater motion through the Lifamatola Passage and its contribution to the Indonesian Throughflow. Deep Sea Res. I, 56:1203-1216, doi:10.106/j.dsr.2009.02.001.

van Aken, H.M., van Bennekom, A.J., Mook, W.G., Postma, H., 1988. Physical aspects of the flushing of the East Indonesian basins. Netherlands Journal of Sea Research, 22:315-339.

Wijffels, S.E., Meyers, G., Godfrey, J.S., 2008. A 20-year average of the Indonesian Throughflow: Regional currents and the interbasin exchange. J. Phys. Oceanogr., 38:1965-1978, doi:10.1175/2008JPO3987.1.

Wolanski, E., Ridd, P. Inoue, M., 1988. Currents through Torres Strait. J. Phys. Oceanogr., 18(11):1535-1545.

Xu, X., Chang, Y., Peters, H., Ozgokmen, T.M., Chassignet, E.P., 2006. Parameterization of gravity current entrainment for ocean circulation models using a high-order 3D nonhydrostatic spectral element model. Ocean Model., 14:19-44.

Yaremchuk, M., McCreary Jr., J., Yu, Z., Furue, R., 2009. The South China Sea Throughflow retrieved from climatological data. J. Phys. Oceanogr., 39:753-767, doi:10.1175/2008JPO3955.1.

Figure captions:

Figure 1: The 1/12° global HYCOM topography (meters) for the subregion of the Indonesian Seas. The three insets (marked with white boxes in the top panel) are for Makassar Strait (bottom left), Lifamatola Passage (bottom middle) and Ombai Strait/Timor Passage (bottom right). The same color bar is used for all panels. Land masses are in italics.

Figure 2: Observed INSTANT (value on the left) and 1/12° global HYCOM (value on the right) mean transport (Sv) for the key passages in the Indonesian Seas over the period 2004-2006. Negative transport is to the south and west and all values are for the full water column except for Lifamatola Passage which is the transport below 1250 m (for both INSTANT and the model). Observations are only available at the five INSTANT mooring locations. Simulated transport is calculated from sidewall to sidewall and the black lines indicate the approximate locations where the model was sampled; these correspond to the INSTANT locations where available. The total ITF is the sum of the three outflow passages: Lombok Strait, Ombai Strait and Timor Passage. Round-off error may cause small discrepancies when summing sections.

Figure 3: Mean 2004-2006 transport per unit depth (Sv) for varying thickness slabs for the INSTANT observations (black lines with x's) and 1/12° global HYCOM (histograms with gray = negative and black = positive) at the INSTANT straits (panels a-b, d-f) and for a section near 2°S from Sulawesi to New Guinea that measures the inflow through the eastern passages (panel c). Panels a,c measure inflow whereas panels d-f measure outflow. Negative transport is southward and westward, i.e. from the Pacific to the Indian Ocean.

Figure 4: Along strait velocity (ASV) (cm/s) vs. depth (m) at Makassar Strait for the INSTANT moorings (solid) and 1/12° global HYCOM (dashed) for the 2004-2006 a) mean and the b)

January-February-March northwest monsoon season (green) and the July-August-September southeast monsoon season (black). Both the observed and simulated profiles are an average of the two moorings and negative values indicate southward flow. The y-axis starts at 25 m, not the surface. The INSTANT profiles are adapted from Gordon et al. (2008). The INSTANT (HYCOM) velocities were rotated to 170° (162°).

Figure 5: Makassar Strait total transport (in Sv) vs. time from the INSTANT moorings (black) and 1/12° global HYCOM (gray) spanning the 2004-2006 time frame. Negative transport is southward. A 10-day running filter has been applied to both time series. The correlation coefficient between the two is 0.74.

Figure 6: The 2004-2006 mean a) along strait velocity (ASV) (cm/s), b) potential temperature (°C) and c) salinity (psu) vs. depth at the Lifamatola Passage mooring site (~127°E, 2°S) from the INSTANT observations (black) and 1/12° global HYCOM (gray). Note the depth range starts at 500 m, not the sea surface. Negative velocities indicate southward flow. The INSTANT profiles are adapted from van Aken et al. (2009). The velocities are rotated to 129° (142°) for INSTANT (HYCOM).

Figure 7: Mean 2004-2006 along strait velocity (cm/s) vs. depth for a) Lombok Strait, b) Ombai Strait and c) Timor Passage from INSTANT (left column) and 1/12° global HYCOM (right column). Note the different scale on the color bars between the upper (0-300 m with a contour interval = .75 cm/s) and lower (>300 m with a contour interval = .25 cm/s) sections with negative values indicating flow into the Indian Ocean. The observed and simulated sections span approximately the same distances. The INSTANT panels are adapted from Sprintall et al. (2009).

Figure 7 continued: Same as for panels a-c except for standard deviation of along strait velocity (cm/s). The color bars are consistent between all panels.

Figure 8: Mean zonal velocity (color filled) and current vectors (m/s) at 100 m around Wetar and Ombai Straits from year 5 of a 1/25° global HYCOM simulation using climatological ECMWF forcing. Blue (yellow-orange-red) colors indicate westward (eastward) flow. Note the flow is all westward across the southern half of Wetar Strait and an east-west section across the strait indicates southward flow at all depths (not shown). The black line corresponds to the location the along strait velocity section in Fig. 7b.

Figure 9: Mean 2004-2006 a) layer 4 and b) layer 9 velocity vectors with speed (m/s) overlain in color from 1/12° global HYCOM for a subregion of the Indonesian Seas. Layer 4 encompasses the approximate depth range of ~20-120 m while layer 9 is at ~150 m across most of the domain. Every third model vector is plotted and the reference vector is .5 m/s.

Figure 10: Mean 2004-2006 layer 9 velocity vectors with speed (m/s) overlain in color from 1/12° global HYCOM in the southern Makassar Strait. Layer 9 is at ~150 m across most of this subregion. Every model vector is plotted and the reference vector is .5 m/s.

Figure 11: Mean 2004-2006 a) January-February-March and b) July-August-September velocity vectors with speed (m/s) overlain in color averaged over layers 20-23 from 1/12° global HYCOM for the area of the western equatorial Pacific Ocean, including Lifamatola Passage (127°E, 1.8°S). Every other model vector is plotted and the reference vector is .1 m/s.

Figure 12: Mean 2004-2006 along strait velocity (cm/s) vs. depth for Timor Passage from 1/12° global HYCOM. This section differs from the one shown in Fig. 7c because it extends farther to the south and includes most of the Australian continental shelf. Note the different scale on the

color bars between the upper (0-300 m) and lower (>300 m) sections with negative values indicating flow into the Indian Ocean.

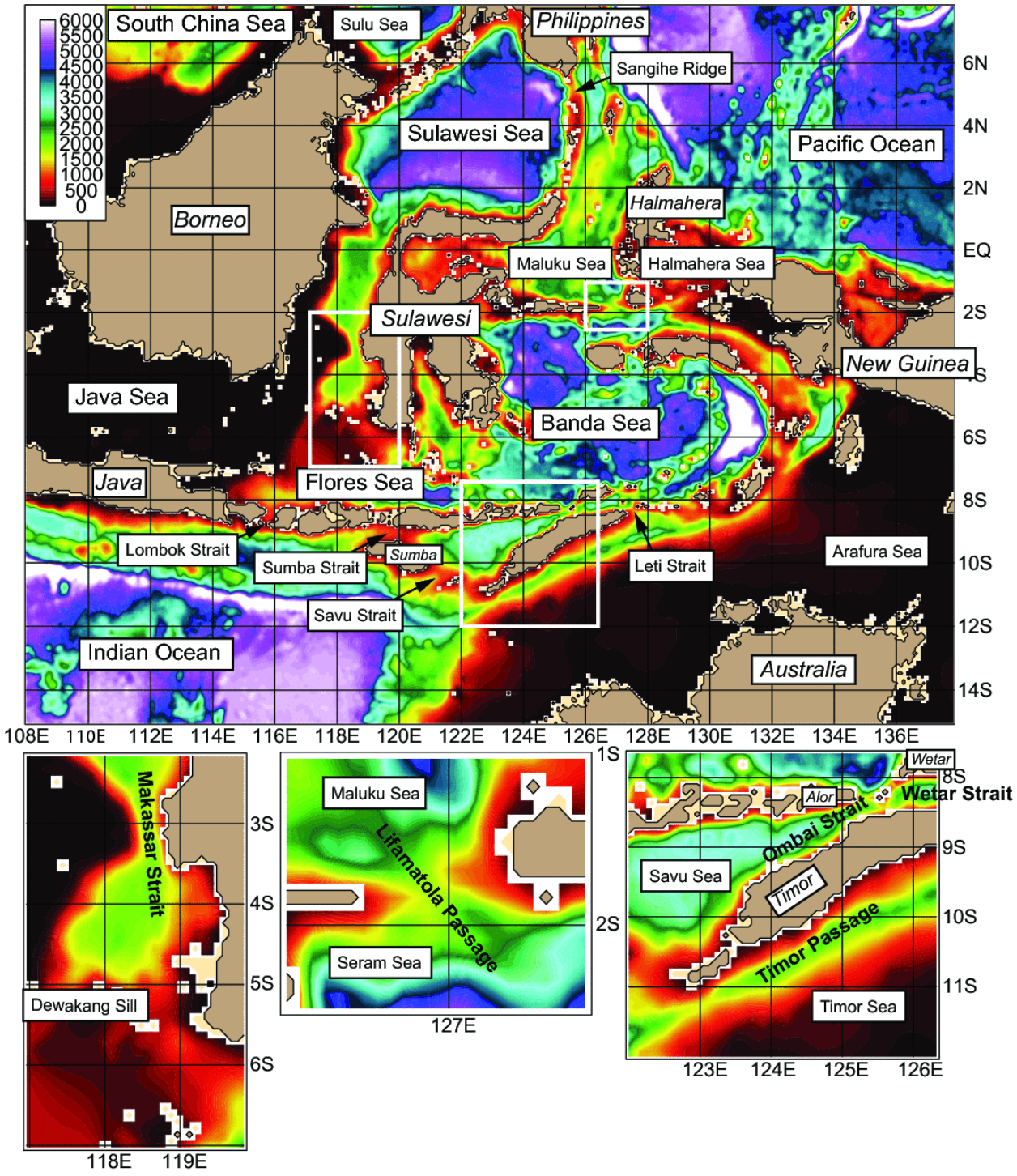

Figure 1: The 1/12° global HYCOM topography (meters) for the subregion of the Indonesian Seas. The three insets (marked with white boxes in the top panel) are for Makassar Strait (bottom left), Lifamatola Passage (bottom middle) and Ombai Strait/Timor Passage (bottom right). The same color bar is used for all panels. Land masses are in italics.

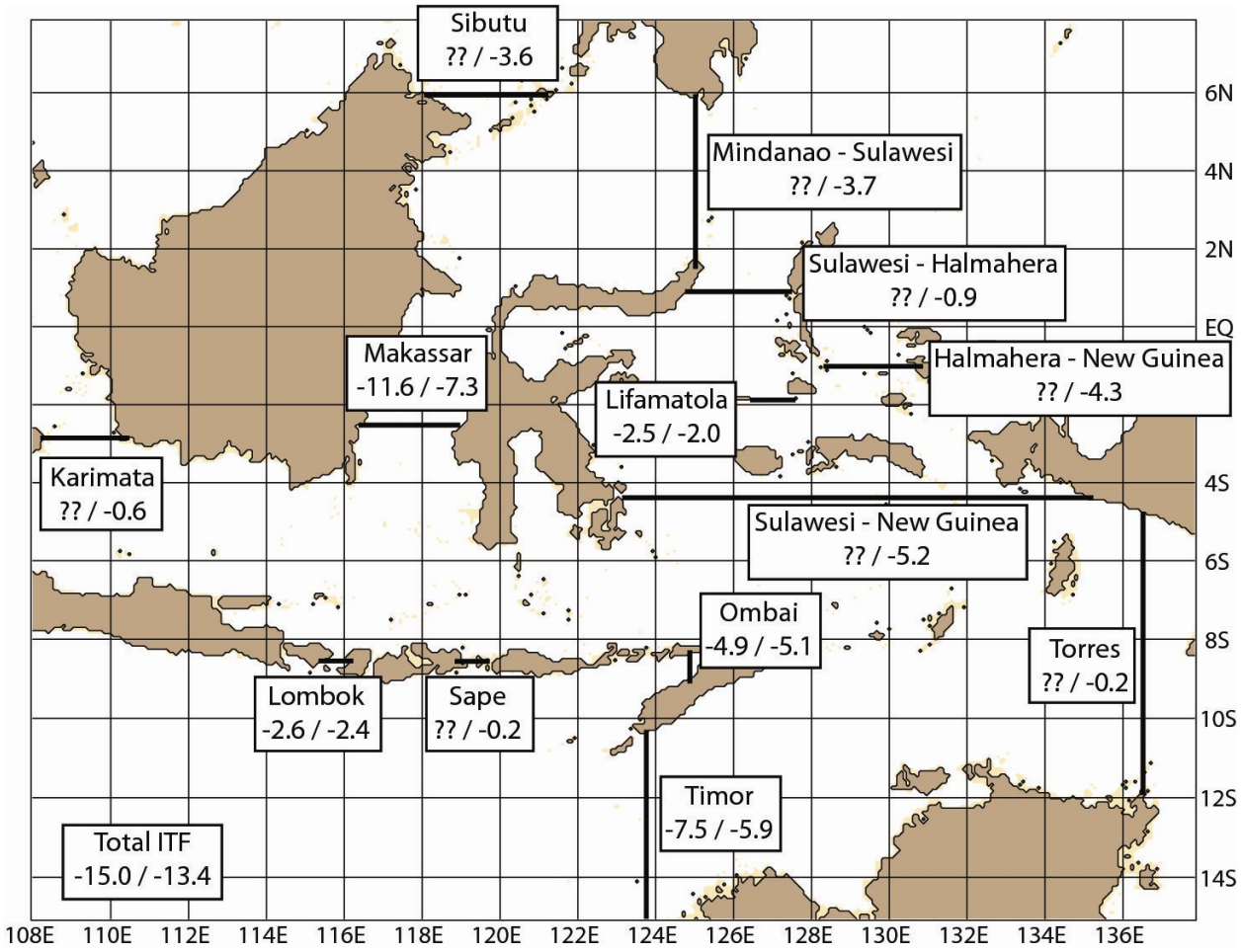

Figure 2: Observed INSTANT (value on the left) and 1/12° global HYCOM (value on the right) mean transport (Sv) for the key passages in the Indonesian Seas over the period 2004-2006. Negative transport is to the south and west and all values are for the full water column except for Lifamatola Passage which is the transport below 1250 m (for both INSTANT and the model). Observations are only available at the five INSTANT mooring locations. Simulated transport is calculated from sidewall to sidewall and the black lines indicate the approximate locations where the model was sampled; these correspond to the INSTANT locations where available. The total ITF is the sum of the three outflow passages: Lombok Strait, Ombai Strait and Timor Passage. Round-off error may cause small discrepancies when summing sections.

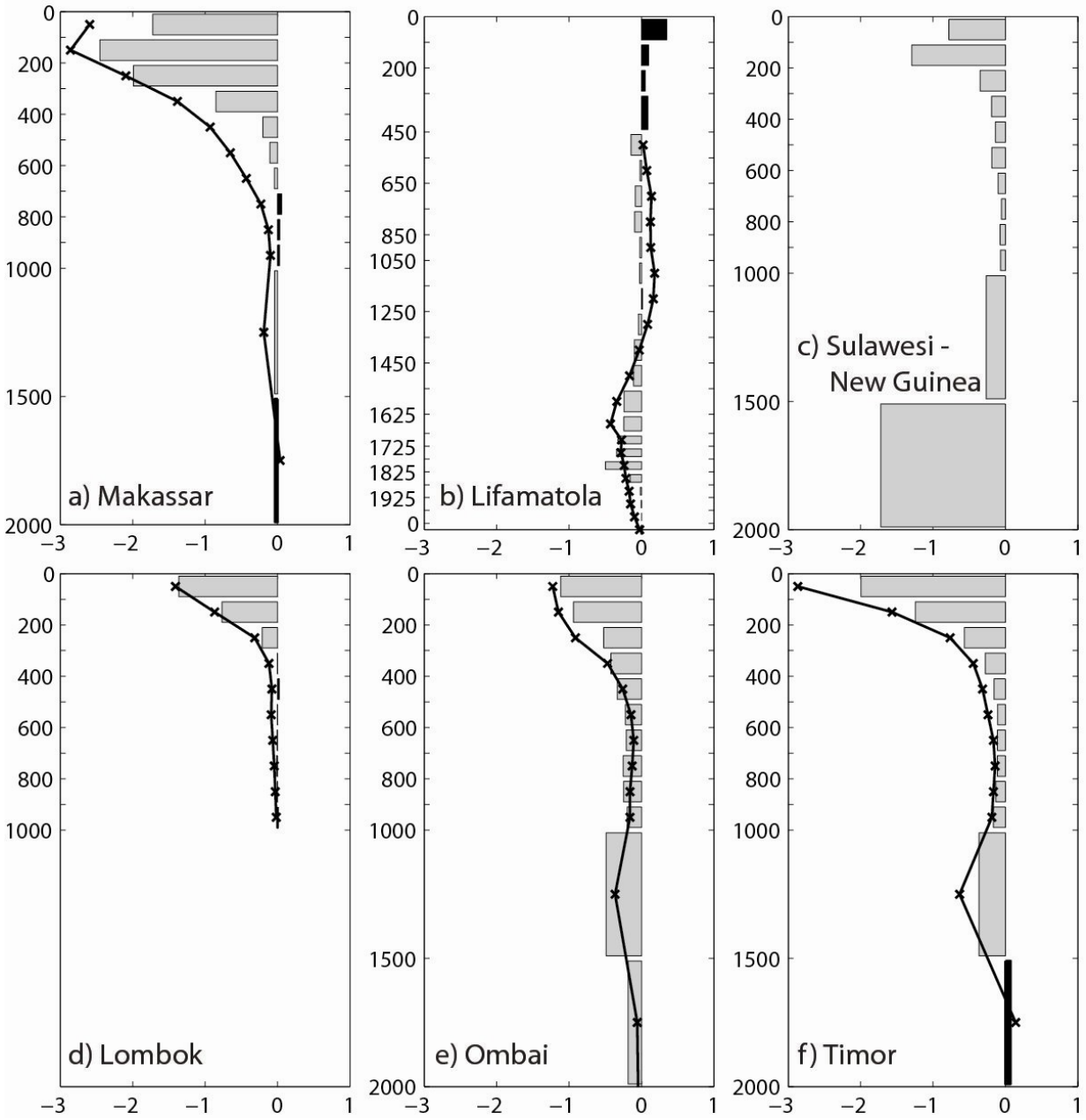

Figure 3: Mean 2004-2006 transport per unit depth (Sv) for varying thickness slabs for the INSTANT observations (black lines with x's) and 1/12° global HYCOM (histograms with gray = negative and black = positive) at the INSTANT straits (panels a-b, d-f) and for a section near 2°S from Sulawesi to New Guinea that measures the inflow through the eastern passages (panel c). Panels a,c measure inflow whereas panels d-f measure outflow. Negative transport is southward and westward, i.e. from the Pacific to the Indian Ocean.

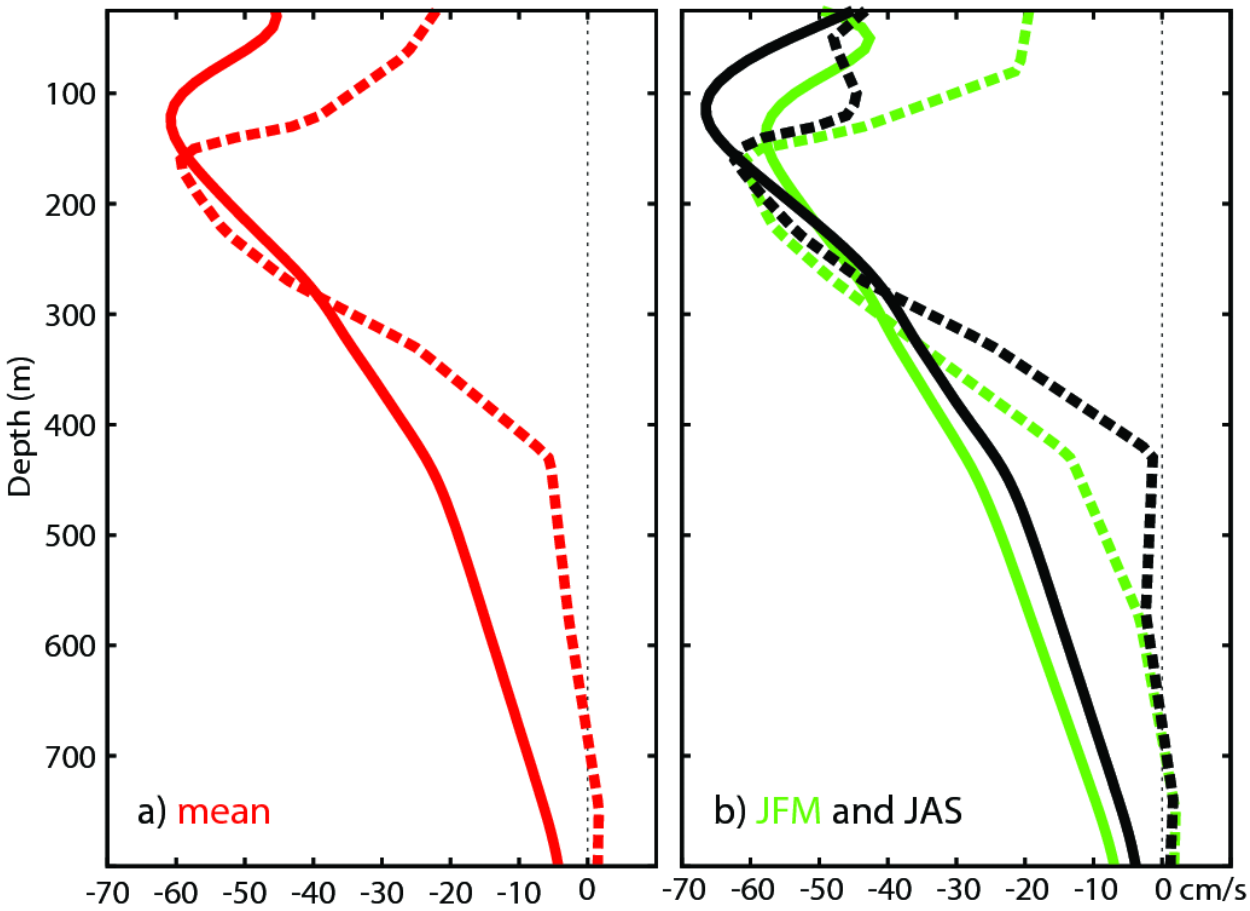

Figure 4: Along strait velocity (ASV) (cm/s) vs. depth (m) at Makassar Strait for the INSTANT moorings (solid) and 1/12° global HYCOM (dashed) for the 2004-2006 a) mean and the b) January-February-March northwest monsoon season (green) and the July-August-September southeast monsoon season (black). Both the observed and simulated profiles are an average of the two moorings and negative values indicate southward flow. The y-axis starts at 25 m, not the surface. The INSTANT profiles are adapted from Gordon et al. (2008). The INSTANT (HYCOM) velocities were rotated to 170° (162°).

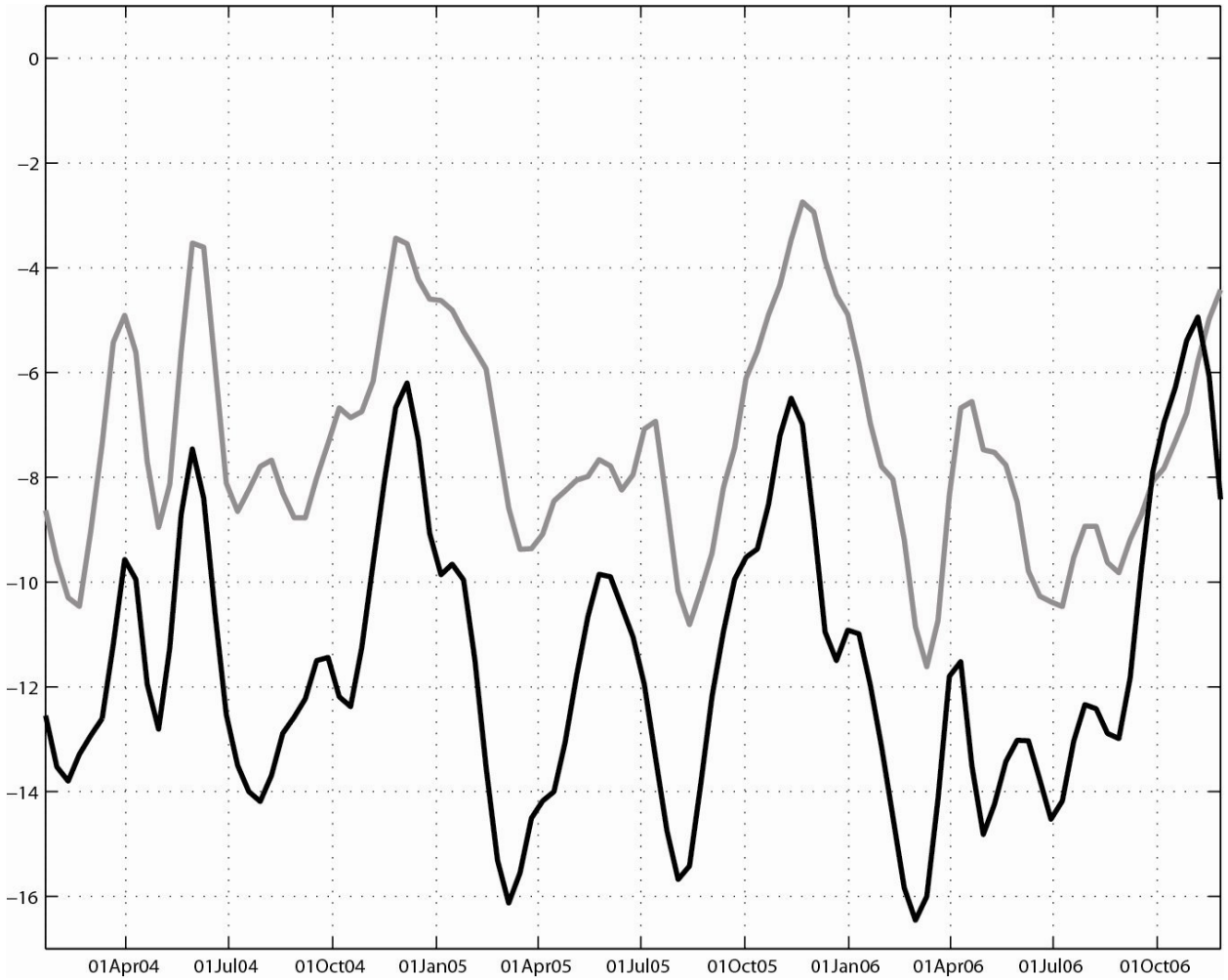

Figure 5: Makassar Strait total transport (in Sv) vs. time from the INSTANT moorings (black) and 1/12° global HYCOM (gray) spanning the 2004-2006 time frame. Negative transport is southward. A 10-day running filter has been applied to both time series. The correlation coefficient between the two is 0.74.

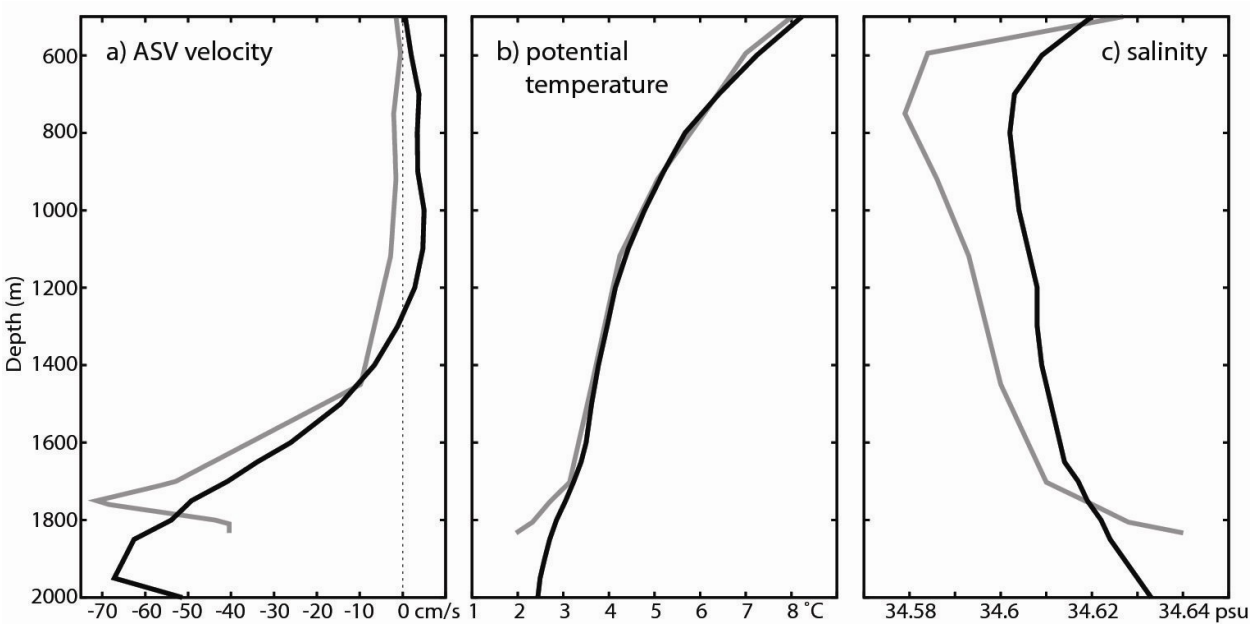

Figure 6: The 2004-2006 mean a) along strait velocity (ASV) (cm/s), b) potential temperature (°C) and c) salinity (psu) vs. depth at the Lifamatola Passage mooring site (~127°E, 2°S) from the INSTANT observations (black) and 1/12° global HYCOM (gray). Note the depth range starts at 500 m, not the sea surface. Negative velocities indicate southward flow. The INSTANT profiles are adapted from van Aken et al. (2009). The velocities are rotated to 129° (142°) for INSTANT (HYCOM).

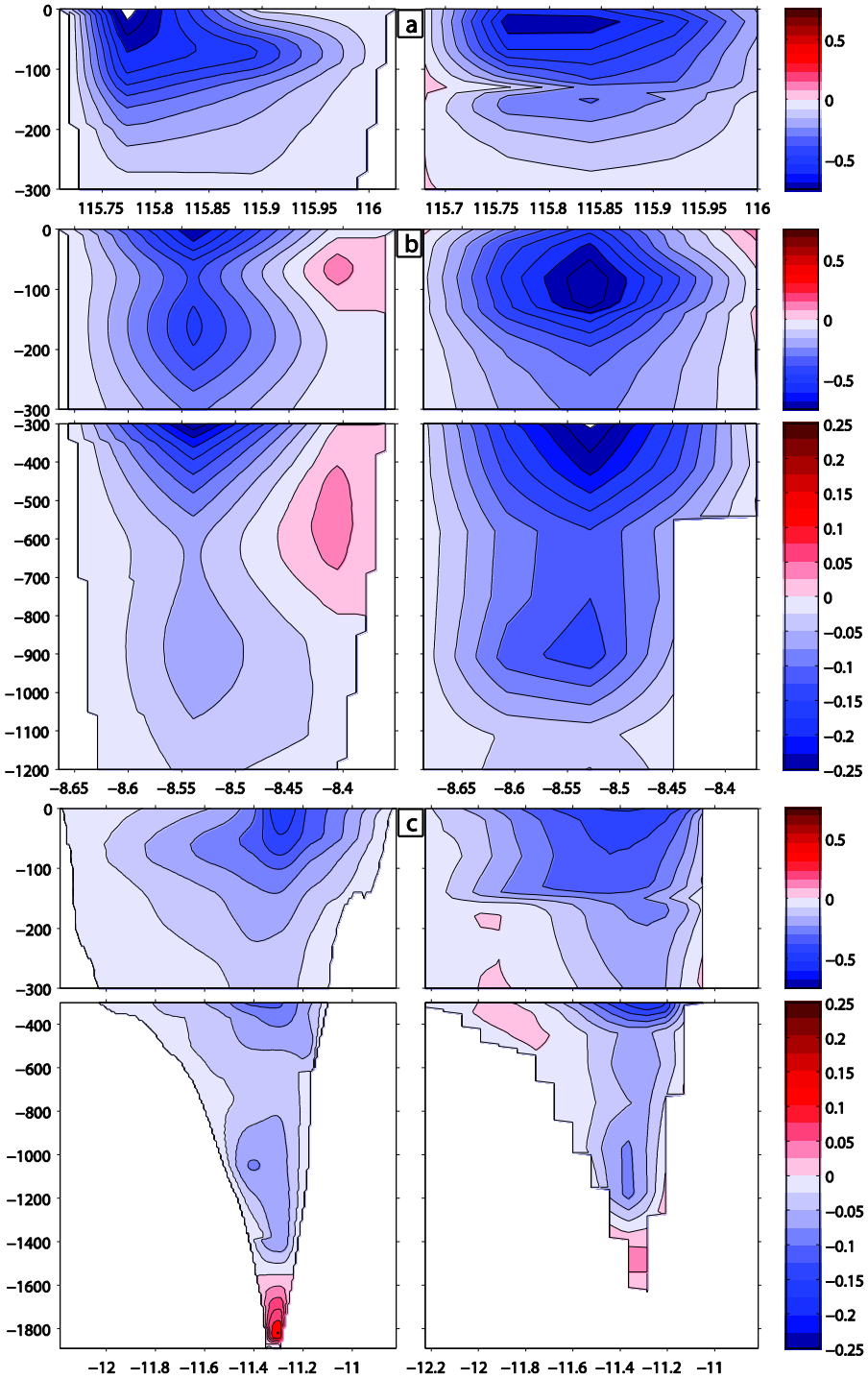

Figure 7: Mean 2004-2006 along strait velocity (cm/s) vs. depth for a) Lombok Strait, b) Ombai Strait and c) Timor Passage from INSTANT (left column) and 1/12° global HYCOM (right column). Note the different scale on the color bars between the upper (0-300 m with a contour interval = .75 cm/s) and lower (>300 m with a contour interval = .25 cm/s) sections with negative values indicating flow into the Indian Ocean. The observed and simulated sections span approximately the same distances. The INSTANT panels are adapted from Sprintall et al. (2009).

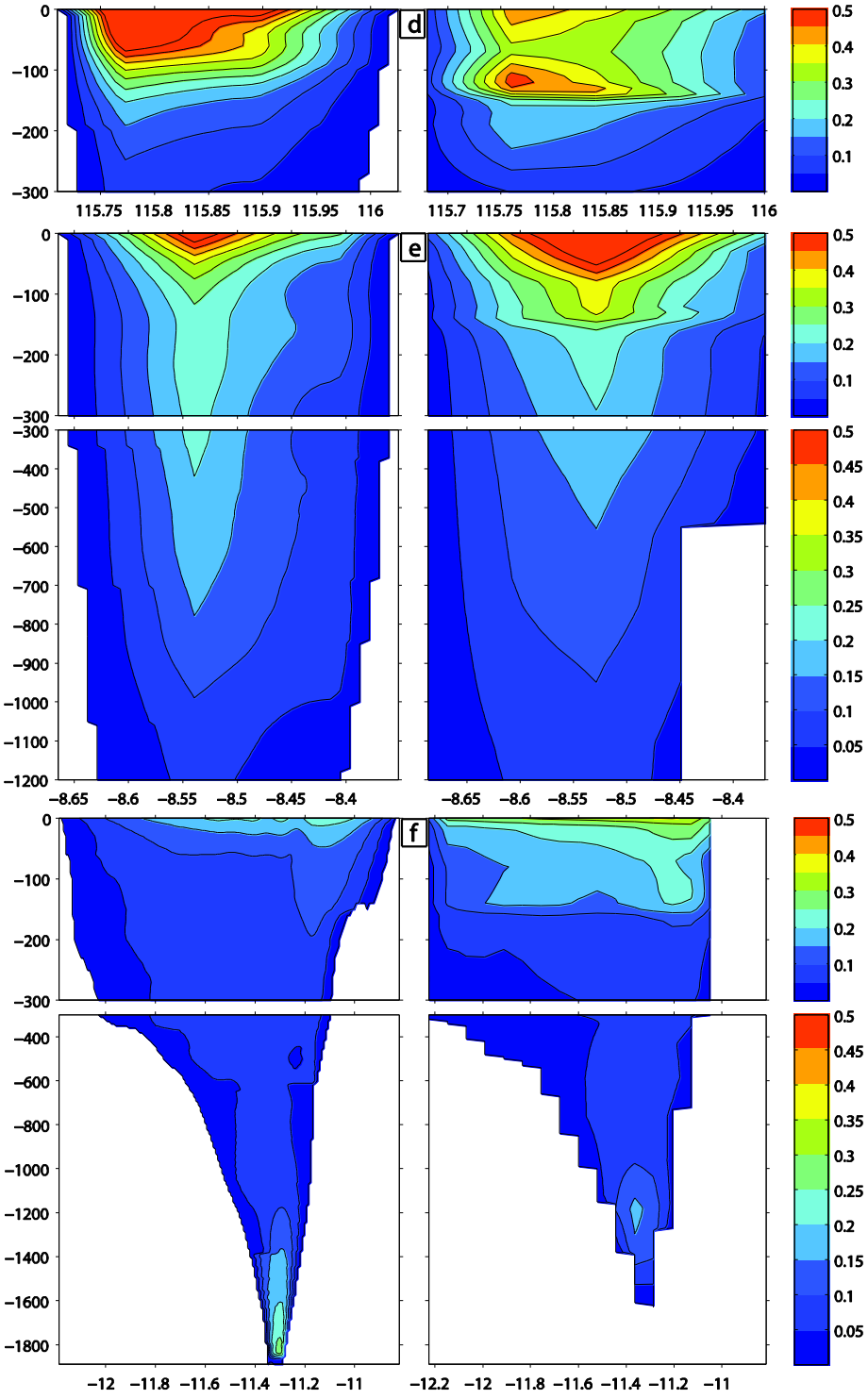

Figure 7 continued: Same as for panels a-c except for standard deviation of along strait velocity (cm/s). The color bars are consistent between all panels.

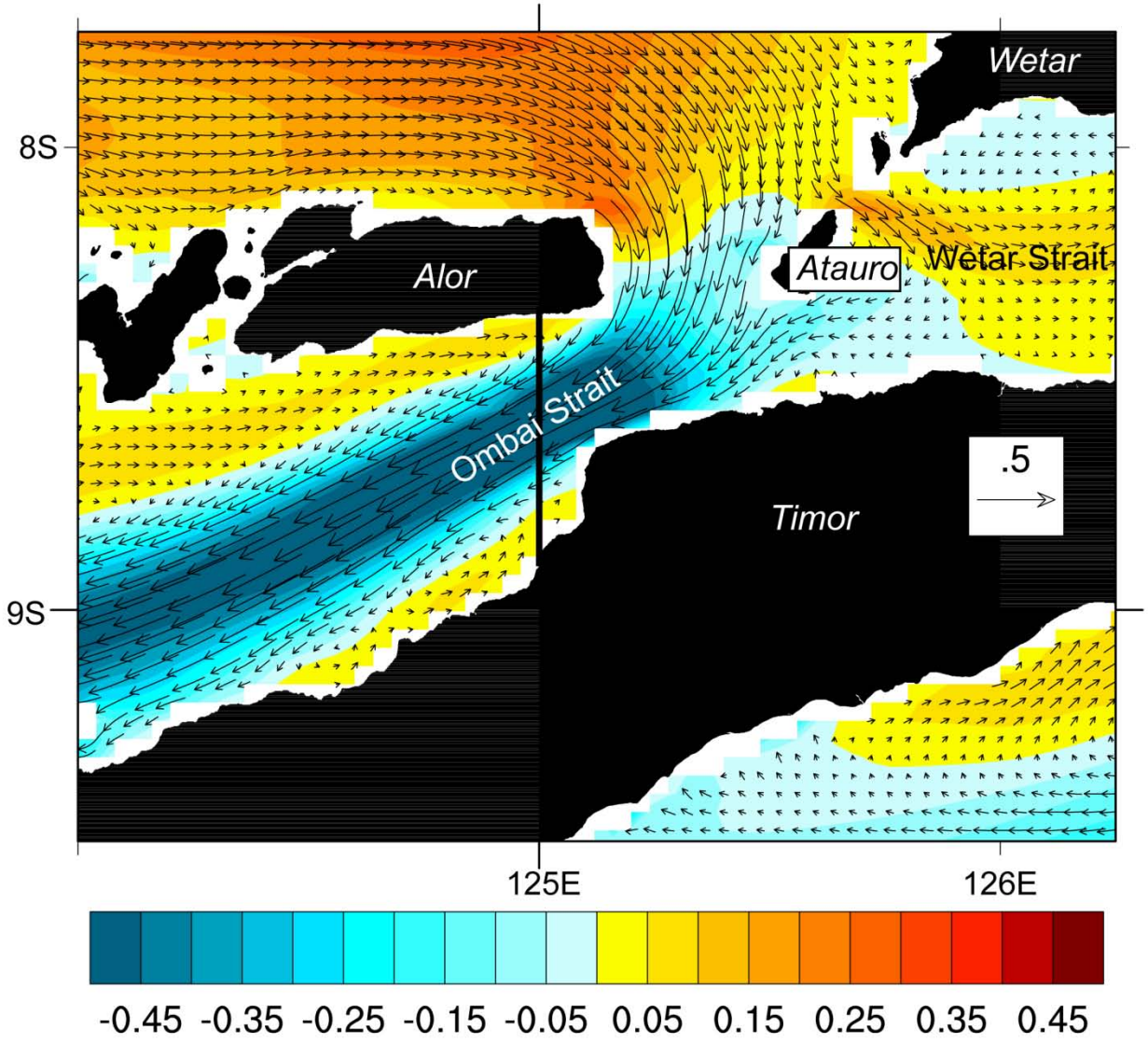

Figure 8: Mean zonal velocity (color filled) and current vectors (m/s) at 100 m around Wetar and Ombai Straits from year 5 of a 1/25° global HYCOM simulation using climatological ECMWF forcing. Blue (yellow-orange-red) colors indicate westward (eastward) flow. Note the flow is all westward across the southern half of Wetar Strait and an east-west section across the strait indicates southward flow at all depths (not shown). The black line corresponds to the location the along strait velocity section in Fig. 7b.

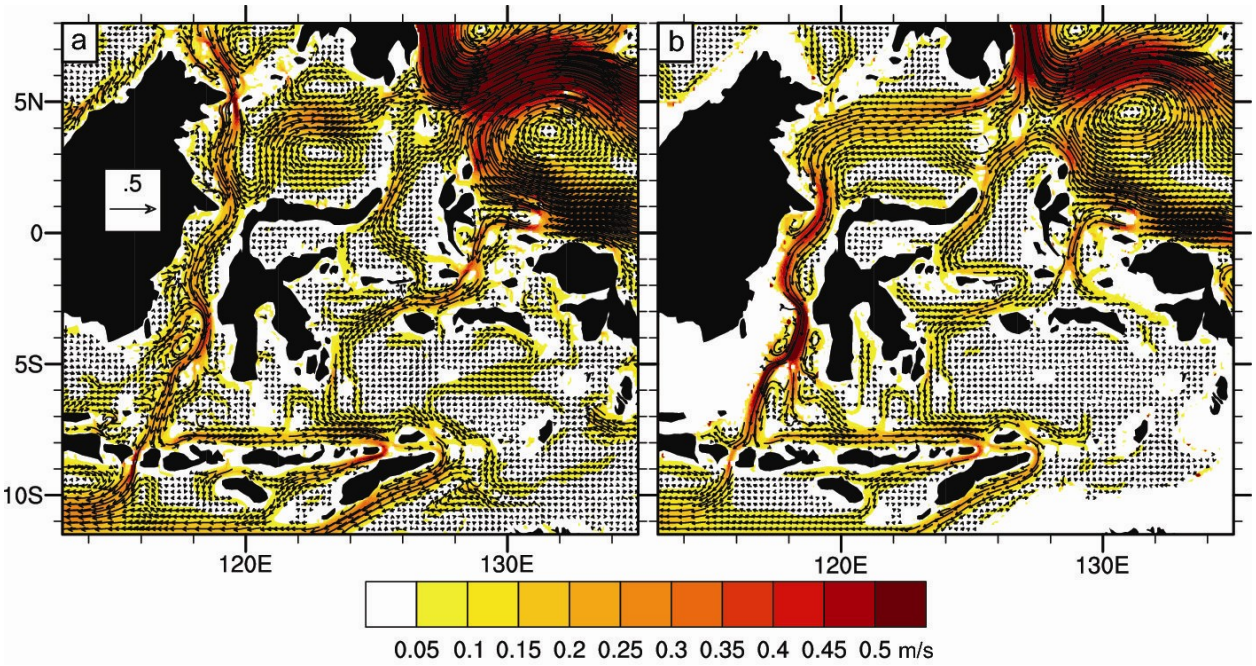

Figure 9: Mean 2004-2006 a) layer 4 and b) layer 9 velocity vectors with speed (m/s) overlain in color from 1/12° global HYCOM for a subregion of the Indonesian Seas. Layer 4 encompasses the approximate depth range of ~20-120 m while layer 9 is at ~150 m across most of the domain. Every third model vector is plotted and the reference vector is .5 m/s.

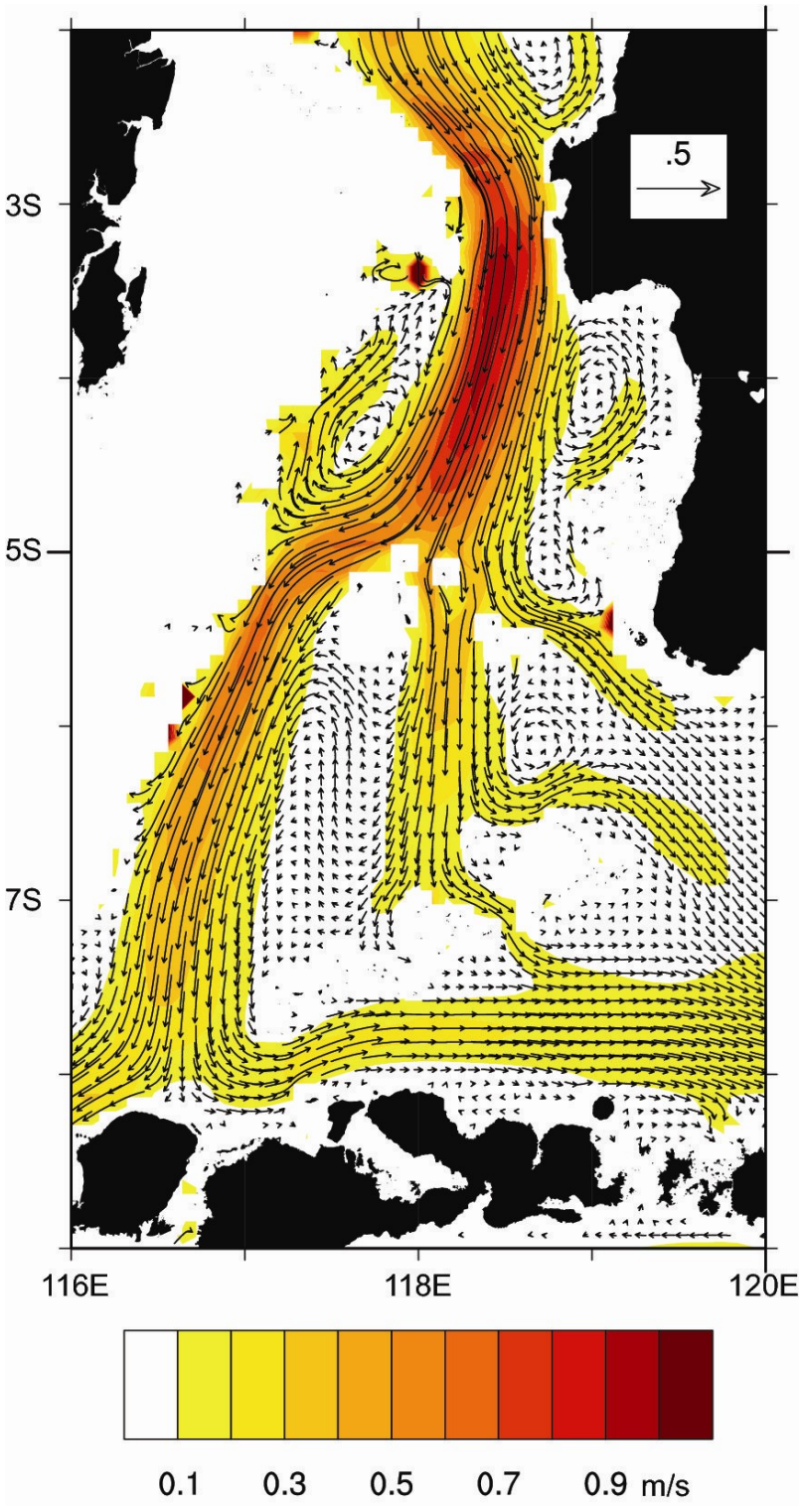

Figure 10: Mean 2004-2006 layer 9 velocity vectors with speed (m/s) overlain in color from 1/12° global HYCOM in the southern Makassar Strait. Layer 9 is at ~150 m across most of this subregion. Every model vector is plotted and the reference vector is .5 m/s.

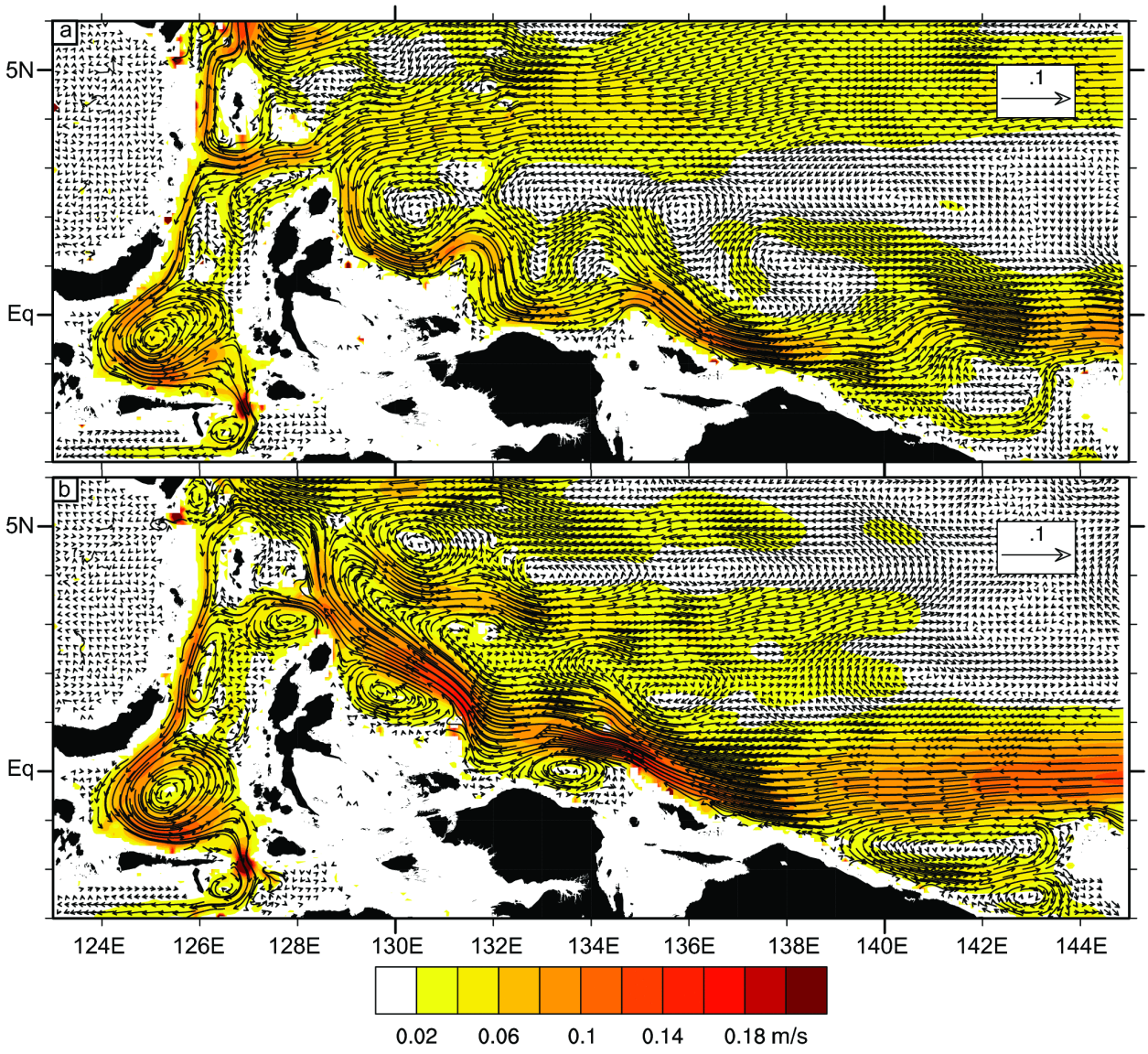

Figure 11: Mean 2004-2006 a) January-February-March and b) July-August-September velocity vectors with speed (m/s) overlain in color averaged over layers 20-23 from 1/12° global HYCOM for the area of the western equatorial Pacific Ocean, including Lifamatola Passage (127°E, 1.8°S). Every other model vector is plotted and the reference vector is .1m/s.

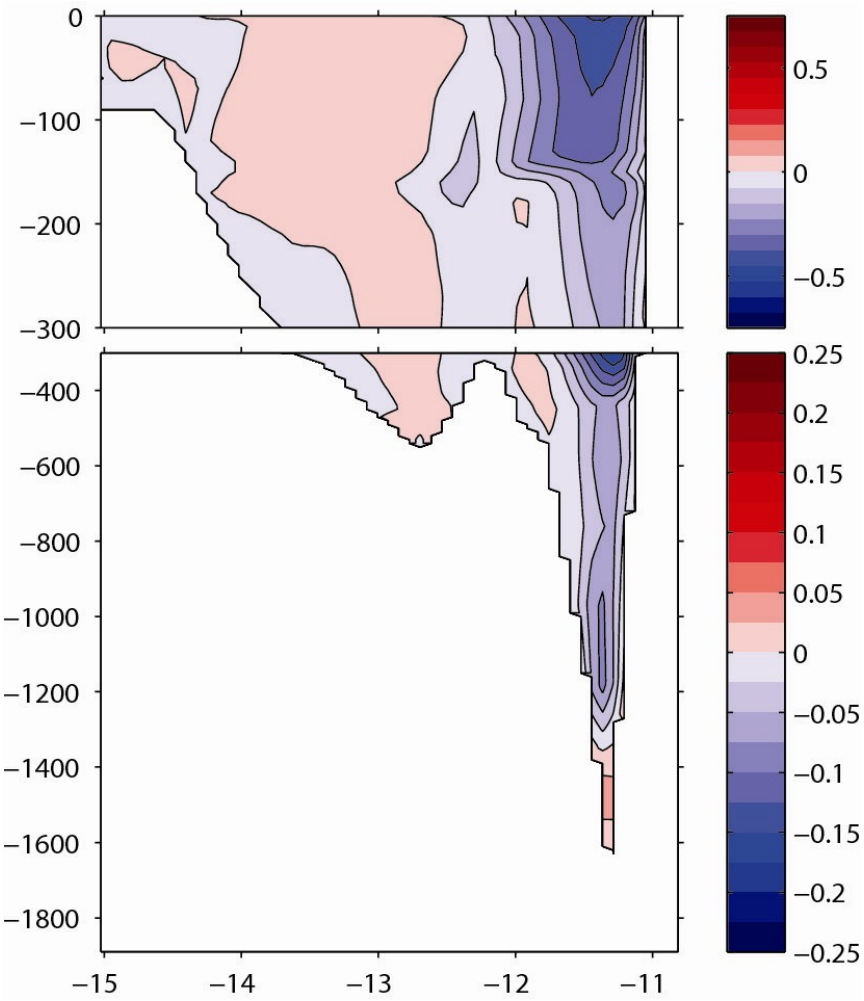

Figure 12: Mean 2004-2006 along strait velocity (cm/s) vs. depth for Timor Passage from 1/12° global HYCOM. This section differs from the one shown in Fig. 7c because it extends farther to the south and includes most of the Australian continental shelf. Note the different scale on the color bars between the upper (0-300 m) and lower (>300 m) sections with negative values indicating flow into the Indian Ocean.